

إن القلب فيه بطنان فقط ولا منفذ بين هذين المنفذين البتة
نفوذ الدم إلى البطن الأيسر إنما هو من الرئة
بعد تسخينه وتصعده من البطن الأيمن.

The blood in the right ventricle of the
heart must reach the left ventricle by way
of the lungs and not through a passage
connecting the ventricles.

[Ibn al-Nafis (d.1288/678). commentary on
the Canon of Medicine by Ibn Sina
(Avicenna)]

Dedicated to

My Father

for his uncompromising principles that guided my life

My Mother

for leading her children into intellectual pursuits

My WIFE

for her magnificent and infinite give and support

My Children

For making everything worthwhile

Aus dem Institut für Physiologie der Medizinischen Fakultät der Charité-
Universitätsmedizin Berlin

DISSERTATION

**Untersuchungen zur Funktion der humanen atrialen
essentiellen leichten Myosinkette (ALC-1) in einem
transgenen Rattenmodell**

Zur Erlangung des akademischen Grades
Doctor medicinae (Dr.med.)

vorgelegt der Medizinischen Fakultät der Charité –
Universitätsmedizin Berlin

Von
Ahmed Ihab Abdelaziz
aus Kairo, Ägypten

Dekan: Prof. Dr. Joachim W. Dudenhausen
Prof. Dr. med Martin Paul

Gutachter: 1. Prof. Ingo Morano, Max-Delbrueck-Center for Molecular
Medicine & Charite University Medicine, Berlin, Germany
2. Prof. Guy Vassort, INSERM Montpellier France
3. Prof. Anders Arner MD, PhD, Lund University Sweden

Datum der Promotion: 20.09.2004

Contents

ABBREVIATIONS		7
LIST OF FIGURES		8
1 INTRODUCTION		10
1.1 Cardiac excitation-contraction-coupling.....		10
1.2 Cardiac myofilament.....		12
1.2.1 Sarcomeric proteins associated with the myofilaments.....		14
1.2.2 Thin filaments.....		16
1.2.2.1 Thin filaments regulation in myocardial contraction...19		
1.2.3 Myosin filaments.....		22
1.2.3.1 Myosin cross-bridges.....		25
1.2.3.2 Myosin cross-bridge cycling kinetics.....		25
1.2.3.3 Myosin heavy chains.....		29
1.2.3.4 Myosin light chains.....		29
1.2.3.5 Regulation of ALC-1 expression in the heart.....		32
1.2.3.6 Functions of ALC-1 in the heart.....		33
1.3 Aim of the study.....		34
2 MATERIALS		35
2.1 Equipments.....		35
2.2 Chemicals.....		37
3 METHODS		40
3.1 Transgene construction and generation of transgenic animals.....		40
3.2 Genotyping of the genomic DNA from the transgenic rat tails.....		40
3.3 Generation of the hALC-1 specific antibody.....		42
3.4 Recombinant human ALC-1 protein.....		42

3.5	Myosin purification.....	43
3.6	Composition analysis of purified myosin and human atrial tissue...	43
3.7	Quantification of the transgene expression.....	44
3.8	Immunofluorescence microscopy.....	45
3.9	Analysis of the ventricular proteome by 2D-PAGE.....	46
3.9.1	Preparation of the protein samples.....	46
3.9.2	2D electrophoresis.....	47
3.9.3	Silver staining, spot detection and mass spectrometry....	47
3.10	Isolated perfused hearts (Langendorff method).....	48
3.11	Statistical analysis.....	49
4	RESULTS.....	49
4.1	Generation and basic characterization of the transgenic rats.....	49
4.2	Quantification of the expressed hALC-1.....	51
4.3	MLC analysis.....	54
4.4	Immunofluorescence microscopy.....	56
4.5	Comparative proteome analysis.....	59
4.6	Functional properties of the transgene.....	61
5	DISCUSSION.....	65
	SUMMARY.....	71
	ZUSAMMENFASSUNG.....	73
	REFERENCES.....	75
	APPENDIX.....	84
	Publications.....	84
	Curriculum Vitae.....	85
	Acknowledgments.....	88
	Erklärung.....	89

ABBREVIATIONS

ADP	Adenosine diphosphate
ALC-2	Atrial regulatory light chain
ATP	Adenosine triphosphate
Ca ²⁺	Intracellular calcium
CaM	Calmodulin
CaMK	Calmodulin dependant kinase
CaN	Calcineurin
CICR	Calcium induced calcium release
+dP/dtmax	maximal rate of pressure increase
-dP/dtmax	maximal rate of pressure decrease
ECC	Excitation-contraction-coupling
F-actin	Filamentous actin
G-actin	Globular actin
GRK	G protein-coupled receptor kinase
hALC-1	Human atrial essential light chain
hALC-1 _{HIST}	HIS-tagged recombinant hALC-1 protein
hAT	Human atrial tissue SDS-extract
HOCM	Hypertrophic obstructive cardiomyopathy
MHC	Myosin heavy chain
MLC	Myosin light chain
MLC-1	Essential myosin light chain
MLC-2	Regulatory myosin light chain
mRNA	Messenger RNA
MW	Molecular weight
MyBP-C	Myosin-binding-protein C
MyBP-H	Myosin-binding-protein H
NCX	Sodium calcium exchange
NHE	Sodium-proton exchanger
P _i	Inorganic phosphate
PKA	Protein kinase A
PLB	Phospholamban
PP	Protein phosphatase

RyRs	Ryanodine receptors
SDS-PAGE	SDS-polyacrylamide gel electrophoresis
SERCA	Sarcoplasmic reticulum calcium ATPase
SR	Sarcoplasmic reticulum
TGR/hALC-1	Transgenic rats overexpressing human atrial essential light chains
Tm	Tropomyosin
Tn	Troponin
T-tubule	Transverse tubular system
VLC-1	Ventricular essential light chain
VLC-2	Ventricular regulatory light chain
V _{max}	Maximal shortening velocity
WKY	Wistar-Kyoto rats

LIST OF FIGURES

Figure 1. Scheme of cardiac excitation-contraction-coupling in ventricular myocyte.....	11
Figure 2. Ultra-structure of the working myocardial cells.....	13
Figure 3. Major components of the cardiac sarcomere.....	15
Figure 4. Thin filaments.....	17
Figure 5. Regulation of thin filament in contraction.....	21
Figure 6. Schematic representation for myosin molecule structure.....	22
Figure 7. Three-dimensional ribbon structure of Myosin S1.....	24
Figure 8. Cross-bridge cycle kinetics.....	28
Figure 9. Schematic representation of the hALC-1 construct.....	41
Figure 10. Genotyping of transgenic rats by PCR.....	49
Figure 11. Heart weight/body weight relationship.....	50
Figure 12. hALC-1 _{HIST} Standard Curve.....	52
Figure 13. Quantification of the expressed hALC-1.....	53
Figure 14. MLC composition analysis.....	55
Figure 15. Immunofluorescence Localization of the transgene-expression.....	57
Figure 16. Expression-patterns of the transgene by immunofluorescence.....	58

Figure 17. Analysis of the ventricular proteome by 2D-PAGE.....	60
Figure 18. Developed left ventricular pressure (LVP).....	62
Figure 19. Maximum rate of pressure increase (+dP/dt max).....	63
Figure 20. Maximum rate of pressure decrease (-dP/dt max).....	64
Figure 21. Amino acid sequence-comparison of the human, mouse and rat ALC-1....	67

1 Introduction

Cardiac contraction is driven by the cyclic interaction of the motor protein type II myosin with the actin filament, consuming ATP as the energy source to produce tension or shortening. Characterization of the functions of myosin and its subunits on the molecular level provides important steps in the understanding of the physiological and pathophysiological states of the heart.

1.1 Cardiac Excitation-Contraction-Coupling

The release of Ca^{2+} from the sarcoplasmic reticulum (SR) following membrane depolarization and subsequent Ca^{2+} -induced myofilament activation is referred to as excitation–contraction coupling (ECC) (Fig. 1). Myocardial contraction is activated by a transient rise in cytosolic free calcium concentration $[\text{Ca}^{2+}]$ to about 1 μM from a resting diastolic $[\text{Ca}^{2+}]$ of about 0.1 μM . Despite a rather modest rise in the average free $[\text{Ca}^{2+}]$, activation of the contractile proteins typically requires the binding of between 40 and 60 μM total Ca^{2+} . The bulk of this Ca^{2+} required for activation of contraction originates from the sarcoplasmic reticulum (SR), with Ca^{2+} influx through L-type Ca^{2+} channels and Na^+ – Ca^{2+} exchangers (NCX) making more minor contributions, although the relative contribution varies between species (Bers 2002).

A central feature of ECC is the gating of SR Ca^{2+} release channels (called ryanodine or RyRs receptors), where gating refers to the opening (or activation) and the closing of individual RyRs channels located within the terminal cisternae of the SR. Gating of RyRs channels is controlled primarily by elevations of $[\text{Ca}^{2+}]$ in the subsarcolemmal space between the T-tubular membrane of the sarcolemma and the terminal cisternae of the SR, which occurs following the opening of sarcolemmal L-type Ca^{2+} channels in response to membrane depolarization (Lopez-Lopez et al. 1994; Lopez-Lopez et al. 1995). The amplification process whereby elevated subsarcolemmal Ca^{2+} ‘triggers’ further Ca^{2+} release from the SR is called Ca^{2+} -induced Ca^{2+} release (CICR).

Relaxation of myocyte contraction involves the extrusion of Ca^{2+} from the cytosol. At steady state, the majority of relaxation involves Ca^{2+} reuptake into the SR by the Ca^{2+} -

ATPase (SERCA2a), with the remaining Ca^{2+} (equivalent to the amount entering via L-type Ca^{2+} channels) being extruded from the myocyte via the NCX (Bers 2002).

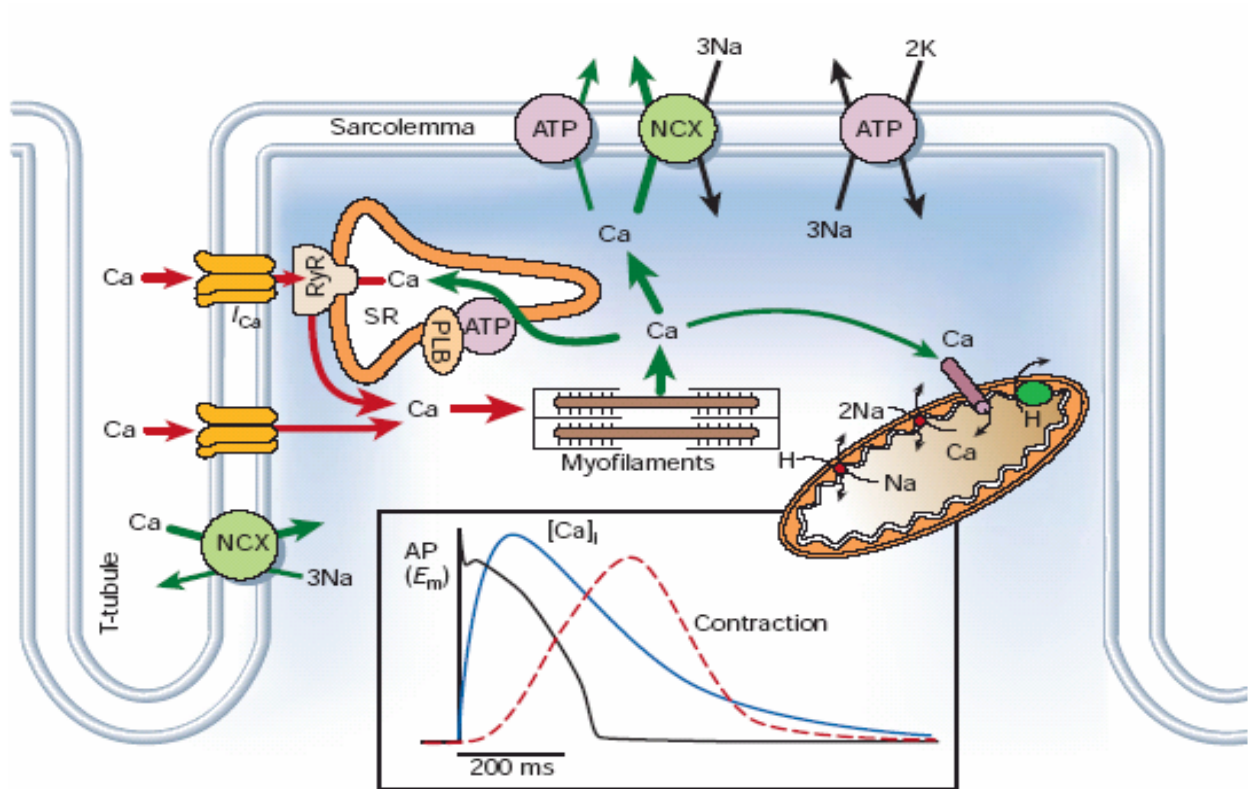


Figure 1. Scheme of cardiac excitation-contraction-coupling events in a ventricular myocyte.

Electrical excitation at the sarcolemmal membrane activates voltage-gated Ca^{2+} channels, and the resulting Ca^{2+} entry activates Ca^{2+} release from the sarcoplasmic reticulum (SR) via ryanodine receptors (RyRs), resulting in contractile element activation. NCX, $\text{Na}^{+}/\text{Ca}^{2+}$ exchange; ATP, ATPase; PLB, phospholamban; SR, sarcoplasmic reticulum. Inset shows the time course of an action potential, Ca^{2+} transient and contraction. (Bers 2002).

1.2 Cardiac myofilaments

Cardiomyocytes contains large number of myofilaments that are organized in a regular array of cross-striations. The cross striations of the myocardium reflect the organization of the contractile proteins into thick and thin filaments. The thick filaments, which are composed largely of myosin, extend the length of the A-band to which they contribute both its darkly staining characteristics and its high birefringence. The thin filaments are composed of actin and the regulatory proteins tropomyosin and troponin complex, they extend the length of the I-bands to which they contribute both its lightly staining striations and less birefringent. A broad dense M-band is found in the center of each A-band, while the I-bands are bisected by Z-lines. The latter delimit the fundamental morphologic unit of striated muscle, the sarcomere, which is defined as the region between two Z-lines. Each sarcomere thus consists of a central A-band plus two adjacent half I-bands. (Fig. 2) (Katz 2001).

During systole the thin filaments are drawn toward the center of the sarcomere by movements of the myosin cross-bridges, which project from the thick filaments to establish bonds with the thin filaments. The thin filaments extend from the Z-lines at either end of the sarcomere into the A-bands, where the extent of overlap between the thick and thin filaments depends on sarcomere length (Katz 2001).

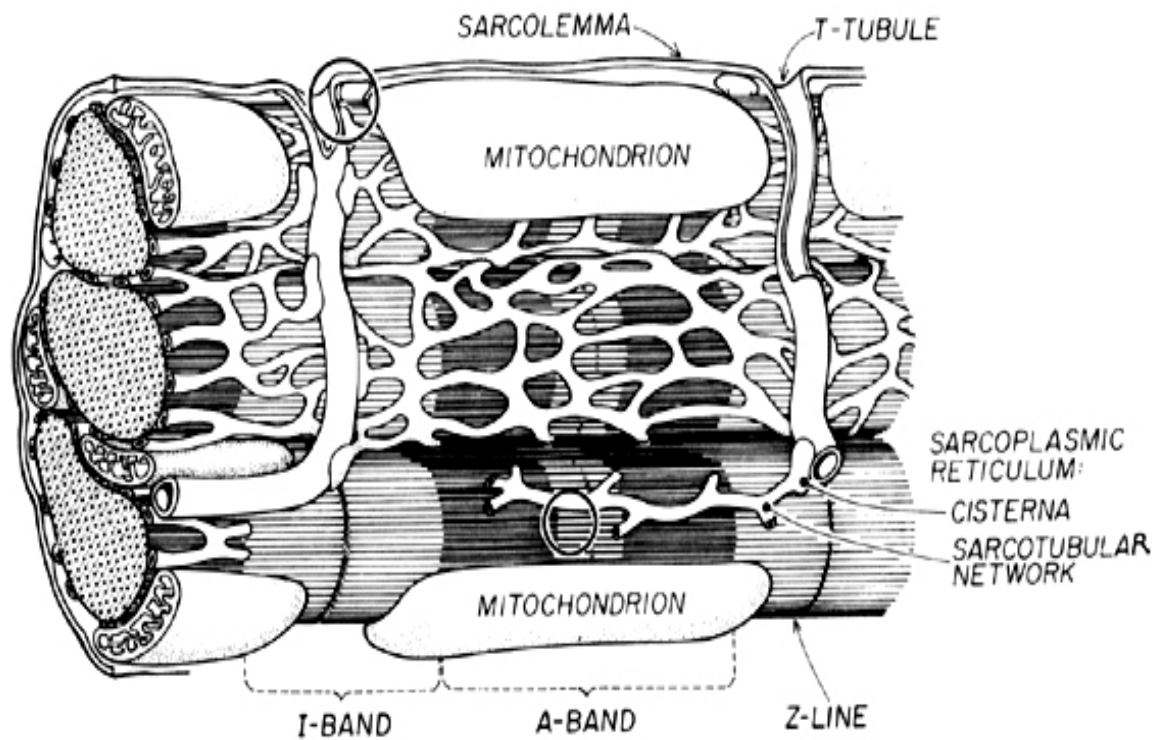


Figure 2. Ultra-structure of the working myocardial cells.

The A-band, the I-band, the Z-lines, the sarcoplasmic reticulum, the transverse tubular system (t-tubule) and the mitochondria are shown in the central sarcomere (see text for explanation) (Katz 2001).

1.2.1 Sarcomeric proteins associated with cardiac myofilaments

Although these proteins do not participate directly in the contractile process, they maintain sarcomere structure and provide mechanical linkages that convey the tension developed by the contractile proteins to adjacent sarcomeres and ultimately to the ends of the muscle (Schiaffino et al. 1996)

At least five proteins are present in the thick filaments contain amino acid sequences that resemble both fibronectin and immunoglobulins (Helmes et al. 1996; Linke et al. 1997; Small et al. 1992). Titin which is also called connectin, is one of the largest known proteins with a molecular weight of about 3,000,000, extends into the thick filaments from the Z-lines (Fig. 3). Titin includes both an elastic region, which is located in the I-band, and a rigid region that supports the thick filaments within the A-bands.

Myosin binding protein C, also called C protein (MW-140,000), which links the thick filaments and titin in the central third of the A-band, plays a role in sarcomere formation (Fig. 3) and contains a number of phosphorylation sites that regulate contractility (Winegrad 1999). Myosin binding protein H (MW-74,000) is present in the Purkinje fibers but not in working cardiac myocytes (Alyonycheva et al. 1997). M-protein and myomesin (MW-185,000) contribute to a set of transverse striations, called M-band, which link the thick filaments in the center of the A-band (Fig. 3). These proteins participate in myofibrillogenesis and stabilize interaction between titin and the thick filaments. Nebulette (MW-107,000) is oriented along the axis of the thin filament and projects from the Z-lines into the I-bands (Moncman et al. 1995). Tropomodulin (MW-43,000) is a capping protein, and is found at the ends of the thin filaments where, by covering the end of the F-actin polymer (Fig. 3), it helps to determine thin filament length (Sussman et al. 1994). α -Actinin (MW-140,000) and Cap Z (β -actinin) (MW-38,000), they weave the ends of thin filaments into the Z-lines at the ends of each sarcomere (Fig. 3).

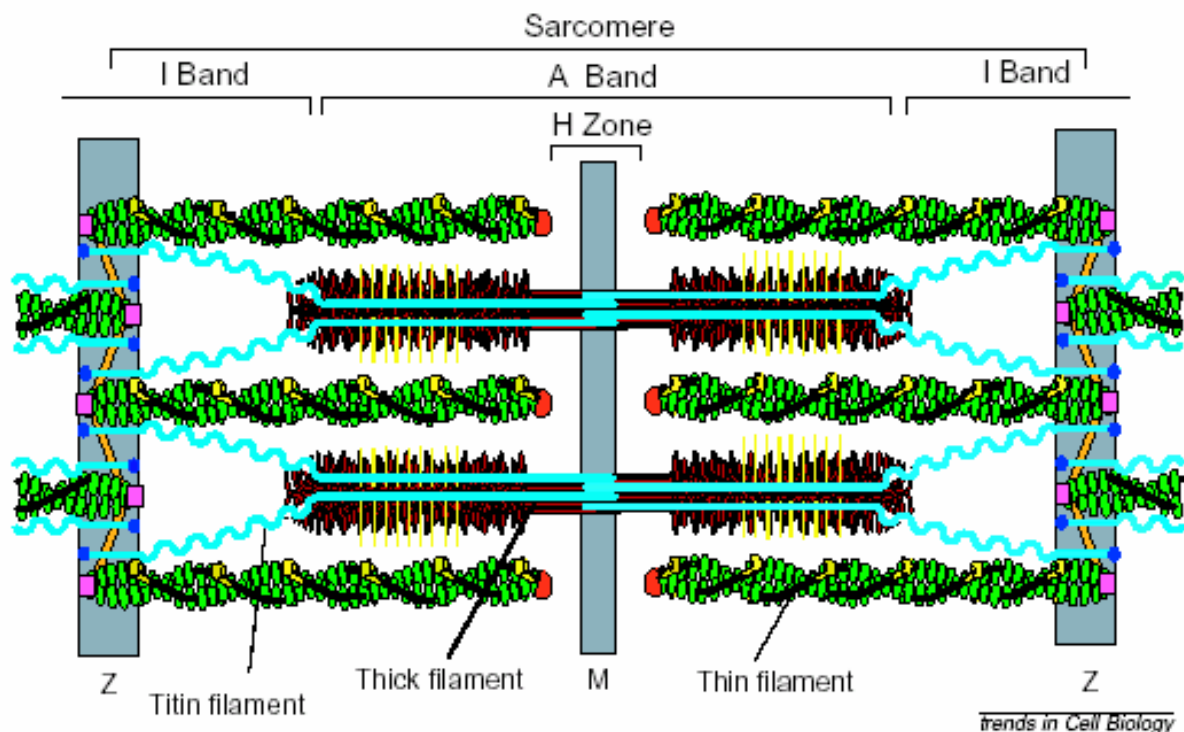


Figure 3. Major components of the cardiac sarcomere:

Actin (green), myosin (red). Rod-like tropomyosin molecules (black lines). Thin filaments in muscle sarcomeres are anchored at the Z-disk by the cross-linking protein α -actinin (gold) and are capped by CapZ (pink squares). The thin-filament pointed ends terminate within the A band, are capped by tropomodulin (bright red). Myosin-binding-protein C (MyBP-C; yellow transverse lines), (Gregorio et al. 2000).

1.2.2 Thin Filament

The main site for Ca^{+2} regulation is the thin filament. Figure 4A is a diagram of the thin filament in striated muscle showing the three components: actin, tropomyosin (Tm), and troponin (Tn) with the three Tn subunits (Gordon et al. 2000).

Monomeric globular actin (G-actin) polymerizes spontaneously to form the backbone of the thin filament, F-actin. The double helical structure of F-actin as two-stranded long-pitch helical structure is evident from electron microscopy of isolated filaments and X-ray diffraction patterns from actin bundles and intact muscle. There are grooves between the two so-called long pitch strands; tropomyosin molecules lie along these grooves such that each tropomyosin molecule interacts with seven actin monomers. There is one troponin complex associated with each tropomyosin molecule (Fig. 4A) (Gordon et al. 2000).

G-actin comprises a single polypeptide chain (mol. Wt 42 000), which binds Ca^{+2} and ATP reversibly. The structure of the actin monomer (Fig. 4B) was determined at atomic resolution (Holmes et al. 1990; Kabsch et al. 1990) into the actin filament helix by modeling against fiber X-ray diffraction patterns from aligned gels of actin filaments (Popp et al. 1987; Popp et al. 1991). The resulting structure is shown in Figure 4B. Each actin monomer comprises four subdomains. Structure positions of subdomains 3 and 4 close to the helix axis, where they interact with subdomains 3 and 4 of other actin monomers. Subdomains 1 and 2 are on the outside of the helix. Subdomain 1 contains the amino and carboxyl termini of the molecule (Holmes et al. 1990).

Tropomyosin (Tm) forms an α helical coiled-coil dimer. Each tropomyosin molecule extends across seven actin monomers in the thin filament and overlaps with neighbouring tropomyosin by about eight residues to form a continuous, rather flexible structure. Image reconstruction studies indicate that tropomyosin lies in the groove of the actin bound to the inner (large) domain of actin (Fig. 4A). One troponin is bound to each tropomyosin dimer, the bulk of the troponin lying about 20nm from the tropomyosin C-terminus (Fig. 4A) (Milligan et al. 1990).

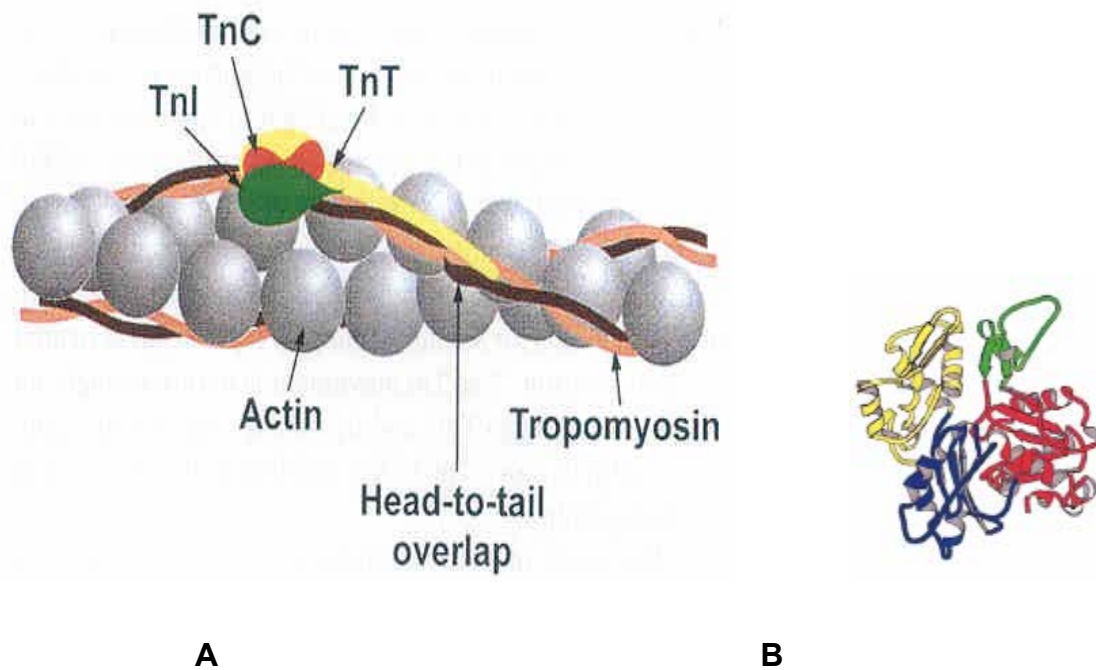


Figure 4. Thin filaments:

(A) A model of the molecular arrangement of troponin (Tn), tropomyosin (Tm), and actin in the cardiac muscle thin filament. The various troponin subunits are indicated [TnC (red), TnT (yellow), and TnI (green)] as they lie along the two-stranded tropomyosin shown (brown) and (orange) that in turn lies along an actin (gray) (Cohen 1975). **(B)** Ribbon diagram (i.e. polypeptide backbone only) of the actin monomer structure subdomains: 1 (red), 2 (green), 3 (blue), and 4 (yellow) (Kabsch et al. 1990).

Troponin comprises three subunits, designated, TnI, TnC, TnT, on the basis of their function. Structural studies showed that Tn belongs to the calcium binding protein family (Kretsinger 1980).

TnC is the myofibrillar protein that by binding Ca^{2+} , transmits the signal to the thin filament. The structure of TnC has been solved to atomic resolution by X-ray crystallography; it consists of two globular domains corresponding to the amino and carboxyl termini, and these are linked by a central, nine-turn α -helix. Each globular domain contains two divalent metal binding sites formed from the helix-loop-helix EF hand motif. The two metal binding sites in the amino-terminal domain are Ca^{2+} specific and are believed to be the regulatory sites (i.e., Ca^{2+} binding to these sites is believed to trigger activation). TnC interacts both with TnI and TnT. TnC interacts more strongly with TnI when Ca^{2+} is not bound to the TnC regulatory sites; modulation of this interaction is believed to be the regulatory mechanism within the troponin complex (Herzberg et al. 1985).

Troponin and tropomyosin exert their regulatory effect in the thin filament by causing inhibition when TnC has no Ca^{2+} bound to the regulatory sites. The actin filament without its regulatory proteins is intrinsically active; that is, it activates myosin ATPase and supports force production and movement. TnI has a major role in inhibiting this activity. In fact, on its own, TnI has an effect on actin filament activity similar to the whole troponin complex at low $[\text{Ca}^{2+}]$. Besides its interaction with TnC, TnI appears to interact with TnT and actin. The interaction with actin is particularly important: it is thought that through this link TnI exerts its regulatory effect and this interaction is modulated by Ca^{2+} binding to TnC (Squire et al. 1998).

TnT is involved in the attachment of the troponin complex to tropomyosin and thus to actin. It is a rodlike molecule with amino and carboxyl termini at opposite ends. The amino-terminal region binds to the head–tail junction of tropomyosin; the carboxyl-terminal region is closely associated with TnC and TnI (Squire et al. 1998).

1.2.2.1 Thin filament regulation in myocardial contraction

Contraction occurs when myosin S1 heads of the thick filament attach to and exert force on actin molecules in the thin filament (Geeves et al. 1999; Xu et al. 1999). This force causes the thin filament to slide over the thick filament and the sarcomere to shorten and develop force against a load. Ca^{2+} binding to troponin (Tn) on the thin filament initiates the force-generating interaction of myosin and actin, and ATP hydrolysis provides the energy for the molecular changes that drive force generation and muscle shortening. Regulation by Ca^{2+} is mediated through changes in the thin filament, although modulation can occur through myosin (Gordon et al. 2001).

Figure 5A shows the salient structural features of thin filament regulation. Helically arranged actins form the backbone of the thin filament, with the regulatory proteins tropomyosin (Tm) and troponin Tn attached to actin in a 7:1:1 (A:Tm:Tn) ratio. Tm, a long, flexible molecule, binds to seven actin monomers in the thin filament helix and overlaps the adjacent Tm. Tn attaches to two actins in the absence of Ca^{2+} through its TnI subunit and to Tm through the TnT subunit.

Ca^{2+} binding to the TnC subunit strengthens the TnC-TnI interaction and detaches TnI from its contacts with actin. Recent structural studies (Vibert et al. 1997) show that this Ca^{2+} -mediated detachment of TnI from actin allows Tm to move over the surface of the thin filament. On the actin surface, there are sites for weak (mainly electrostatic) and strong myosin binding (Fig. 5A). Tm either rolls around its axis or slides from a position near the outer edge of the thin filament [where it covers many of the myosin binding sites on actin (Fig. 5B)] to a position allowing increased weak and some strong myosin head binding (Fig. 5C). Tm is a flexible molecule, and its positioning should be considered dynamic; Tm does not occupy a single fixed position in the presence of elevated $[\text{Ca}^{2+}]$ but “rocks and rolls” or “slips and slides” back and forth over the actin surface. The Tm positions (Fig. 5, B–D) should therefore be considered average positions. When myosin cross-bridge is strongly bound to actin, Tm is locally stabilized in a position that makes both weak and strong myosin binding sites available on nearby actin monomers (Fig. 5D).

Thus structural data suggests that thin filament activation is achieved by the movement of Tm over the actin surface, which is controlled both by Ca^{2+} binding to TnC and initial cross-bridge binding to actin to allow additional strong cross-bridge binding. This Tm motion permits force generation and shortening (Gordon et al. 2001).

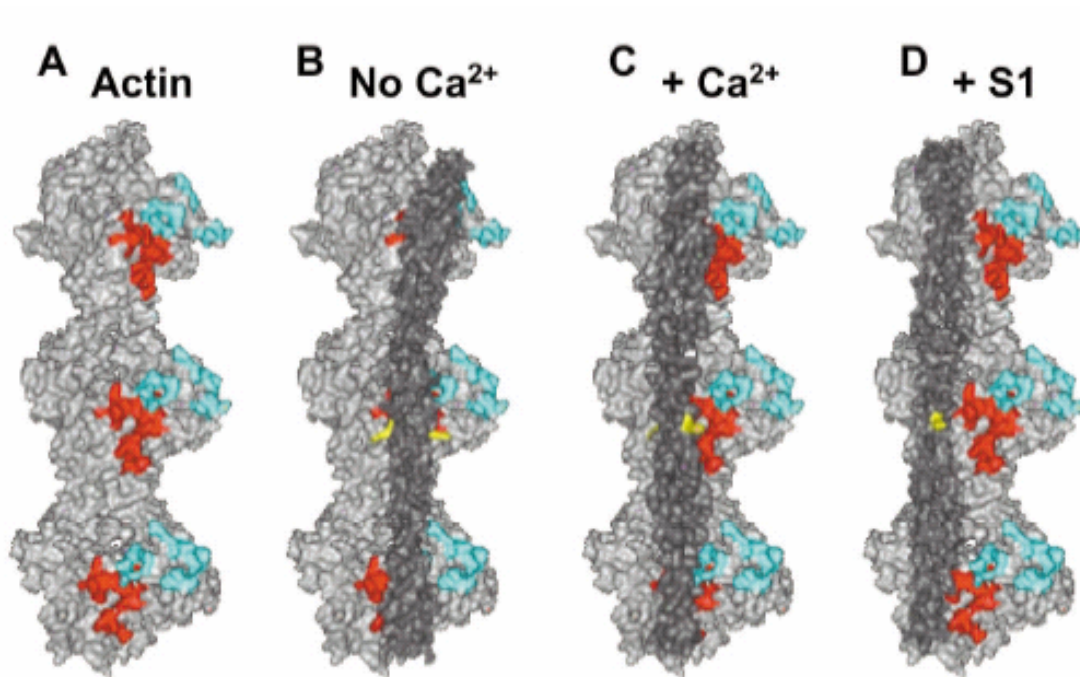


Figure 5. Regulation of thin filament in contraction

Actin residues are light gray, except for residues (1–4, 24–25, 95–100; shown in light blue) making weak electrostatic interaction with myosin and residues (144–148, 340–346, 332–334; shown in red) forming stronger attachments with myosin. In B–D, a surface rendering of a cardiac tropomyosin segment (residues 61–112 of each tropomyosin strand) in dark gray. Arg90 of tropomyosin in each strand is shown in yellow to illustrate the putative rolling motion of tropomyosin. (Gordon et al. 2001).

1.2.3 Myosin filament

The motor protein, myosin II, is composed of two heavy chains with molecular masses of 200 kDa each and four light chains, two each of so called essential and regulatory light chains (MLC 1 and MLC 2, respectively), of molecular mass 20 kDa. The heavy chains form a parallel two-chain coiled-coil structure over most of their length except for the large, globular NH₂-terminal regions, termed heads or S1 (subfragment 1). One pair of light chains bind to each S1. The coiled-coil region of the myosin, termed the myosin rod (tail). The S1 head structure projecting from the backbone of the thick filament interacts with actin to generate force and filament sliding (Fig. 6) (Sellers et al. 1995).

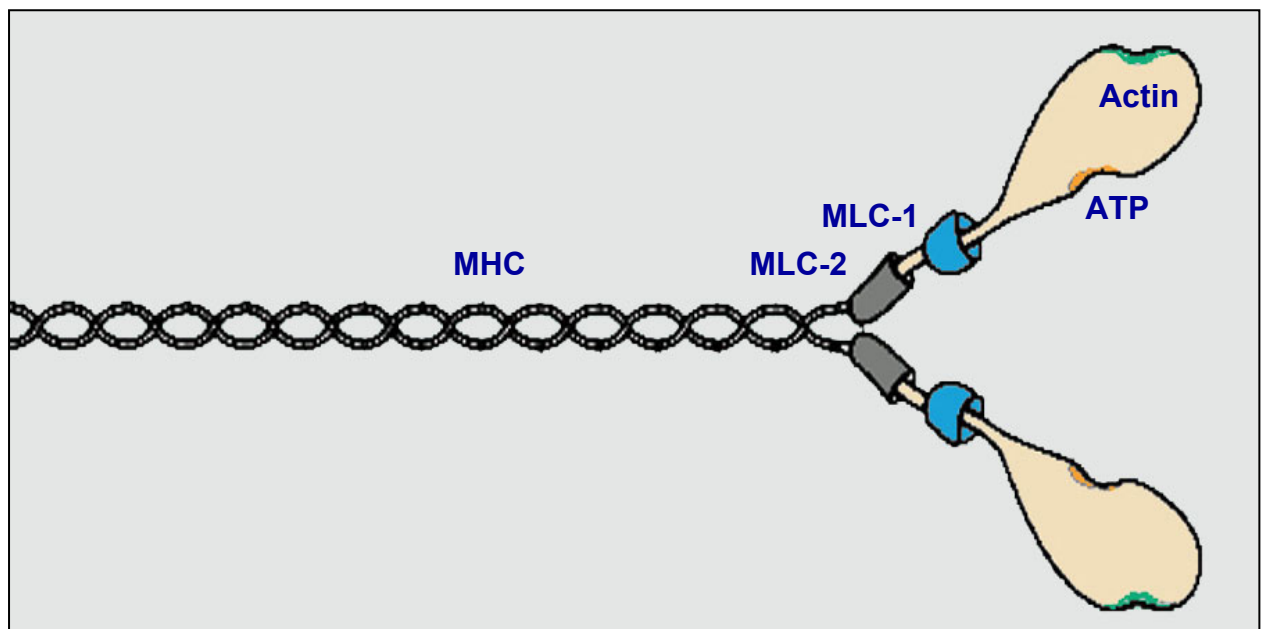


Figure 6. Schematic representation for myosin molecule structure:

The myosin heavy chains (MHC) have a globular "head" with the ATP and actin binding sites at the amino terminal and a long α -helical "tail" at the carboxy terminal. The essential myosin light chain (MLC-1) and the regulatory myosin light chain (MLC-2) at the neck region.

Limited proteolysis of S1 reveals three major segments, a 25-KDa N-terminal, a central 50-KDa and a 20-KDa C-terminal domain (Mornet et al. 1979). The three dimensional structure of the S1 domain of the myosin molecule has been elucidated by X-ray crystallographic analysis (Fig. 7) (Rayment et al. 1993). It consists of a heavy chain (MHC) which folds at the N-terminus into an asymmetric globular head domain. This head is 16.5 nM long, 6.5 nM wide, and 4 nM thick and comprises a seven-stranded β -sheet connected by flanking α -helices and /or loops which constitute the catalytic domain.

The 50-KDa domain is split by a long narrow cleft with actin-binding sites located on both sides of the cleft. Also the ATP-binding (active) site forms an open cleft and is located opposite to the actin-binding site at the 25/50 KDa junction. The apex of the long cleft through the 50 KDa domain is very close to the nucleotide binding cleft, thus mediating signal transduction between the actin and nucleotide binding clefts.

Amino acids 771-843 at the C-terminus form an 8.5 nM α - helical structure, the neck region that binds two types of light chains. The essential myosin light chain binds between amino acid 783 and 806 and the regulatory light chains further downstream between amino acids 808 and 842. A so-called converter domain joins the catalytic and light chain binding domains (around amino acids 711-771).

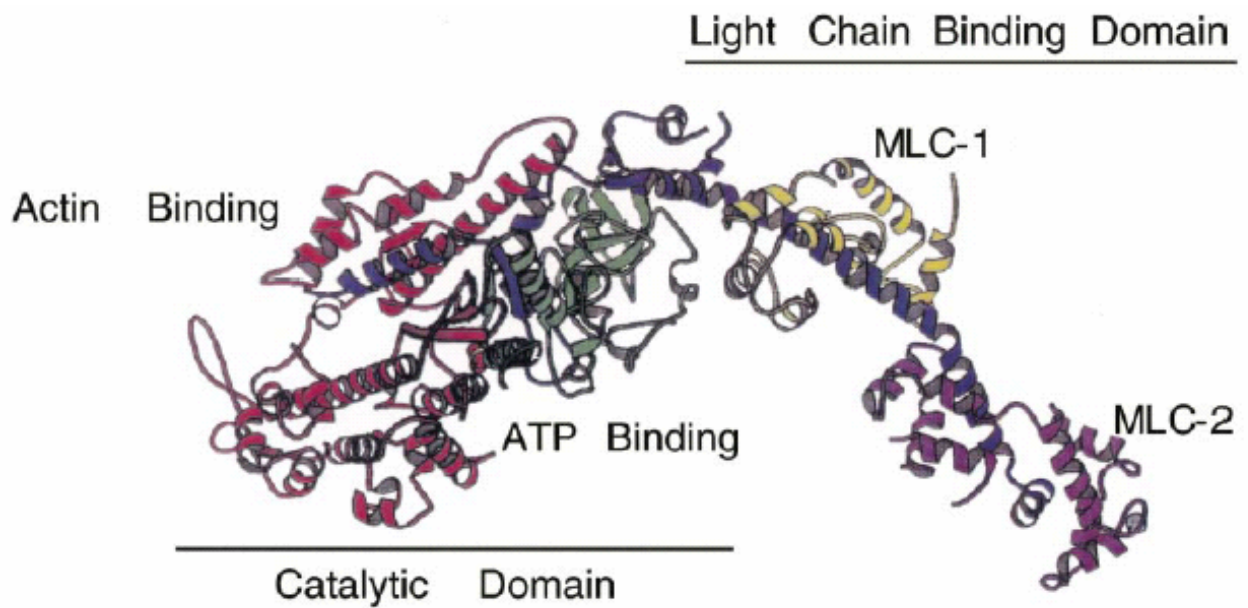


Figure 7. Three-dimensional ribbon structure of Myosin S1 (Rayment et al. 1993). The MHC consists of a 25-K N-terminal (green), a 50-K (red), and a C-terminal joining 20-K (blue) domain. The pear-shaped head is called the catalytic domain. Essential MLC-1 (yellow) and regulatory myosin light chain MLC-2 (magenta) are associated with the α -helical C-terminal part of the 20-K domain (light chain binding domain)

1.2.3.1 Myosin cross-bridge

The swinging-cross-bridge hypothesis of muscle contraction (featured in most text books) was recently modified into swinging-lever arm hypothesis in which the bulk of the cross-bridge is envisaged to bind to actin without rolling on the surface during the power stroke (as had been initially suggested); large movements are envisaged as coming from the distal (C-terminal) part of the myosin cross-bridge moving as a lever arm (Geeves et al. 1999).

The structural changes in the cross-bridges are associated with the strain of an elastic component present in the cross-bridges, which operates over a range of 8–10 nm (Huxley et al. 1971). The α -helical neck domain is believed to function as a lever arm which swings relative to the catalytic domain: picometer changes in the active site of S1 are magnified into nanometers of motion by rotation of the converter domain (Eisenberg et al. 1985; Holmes 1997). In fact, truncation and elongation of the light chain binding domains show that the sliding velocity of actin filaments is proportional to the length of the lever arm (Uyeda et al. 1996). Furthermore, the light chain binding domain, rather than the catalytic domain, reveals tilting motions during length perturbations of an isometrically contracting muscle (Hopkins et al. 1998; Irving et al. 1995; Lombardi et al. 1995). The elastic element of the cross-bridge may therefore reside in the lever arm (Howard et al. 1996).

1.2.3.2 Cross-bridge cycle kinetics

In the intact contractile structure the ATP- or ADP-Pi- loaded MHC binds (as the cross-bridge) to the N-terminus of actin. Myosin undergoes changes in actin affinity and structure, being strongly attached to actin (having high affinity) or weakly attached (having low affinity) (Brenner 1988; Eisenberg et al. 1985). Force is generated upon the transition from the weakly to the strongly attached state. This transition is considered to be coupled to the Pi release step (Dantzig et al. 1992). Figure 8 shows the structural and biochemical events in a cross bridge cycle (Gordon et al. 2001):

Step 1: At physiological ATP concentrations (3–5 mM), ATP binding to myosin is very rapid and irreversible.

Step 2: The subsequent detachment of actin from the actin-myosin-ATP (A~M-ATP) complex is similarly rapid and is caused by an opening between myosin's upper and lower 50-kDa regions like the opening of jaws.

Step 3: A “flexing” or bending of the myosin neck region accompanies the hydrolytic cleavage of ATP, whose equilibrium constant (K_3 , defined as k_{+3}/k_{-3}) is only ~ 10 .

Step 4: Following ATP cleavage, myosin again binds weakly to actin at a high rate, but in the absence of Ca^{2+} Tm sterically blocks access of the myosin head to strong binding sites on actin (Fig. 8B). However, when Ca^{2+} is bound to TnC, TnI detaches from actin, allowing the Tm/Tn complex to roll or slide over the thin filament surface. This exposes weak binding sites on actin and transiently exposes strong binding sites on actin (Fig. 8B) for binding to the complementary regions in myosin's 50-kDa domain.

Step 5: The greater the $[\text{Ca}^{2+}]$, the greater the fraction of time the Tm/Tn complex allows myosin access to strong binding sites on actin. Consequently, the rate of strong cross-bridge attachment, the flux through is dependent on $[\text{Ca}^{2+}]$ and Tm position (i.e., in the simplest case, the value of k_{+5} is proportional to the fraction of Tn having bound calcium). Strong binding of myosin to actin (Fig. 8B) is associated with movement of the upper and lower 50-kDa subdomains toward each other (or closing the jaws). This movement may allow the neck region of myosin to extend, opening a pathway for inorganic phosphate release from the ATP binding pocket in myosin. Alternatively, closing the jaws might promote inorganic phosphate release from the binding pocket, which then allows the extension of myosin's neck region.

Step 6: In any event, myosin neck extension is the power stroke that, in isometric muscle, stretches an elastic element by some 10 nm and produces force. In nonisometric conditions, shortening of the neck extension causes the thick and thin filaments to slide past each other.

Step 7: Is an irreversible isomerization and is strain sensitive; i.e., when the force on the cross-bridge is large as in isometric contractions, k_{+7} is slow (3–10 s⁻¹) and is the rate-limiting step for the cross-bridge cycle. Finally, ADP is released from A·Mf·ADP (where f is a cross-bridge exerting force).

Step 8: Is reversible to form the rigor state, A·Mf. During isometric contractions, the slowness of k_{+7} causes the population of cross-bridges in the initial force-bearing (A·Mf*·ADP) state to rise and with it force.

Cross-bridges attach and exert force constantly during steps 7, 8, and 1 during isometric contraction, and force drops to zero when the cross-bridges detach in step 2. During shortening contractions the filaments slide past each other, the strain on the cross-bridge is reduced, and step 7 occurs more rapidly. This accounts for the Fenn effect (an increased rate of energy liberation above the isometric rate as shortening velocity increases). The chemomechanical mechanism shown in figure 8 implies that during an isometric contraction, a cross-bridge remains strongly attached to actin for a relatively long time (>100 ms/cycle). Strongly bound cross-bridges prevent Tm/Tn from returning to its blocked or closed position, maintaining the thin filament in a “switched on” position (Fig. 8B). In the absence of Ca²⁺, cross-bridge detachments at the end of the cycle allows Tm/Tn to cover the strong myosin binding sites on actin and deactivate the thin filament (Fig. 8A)

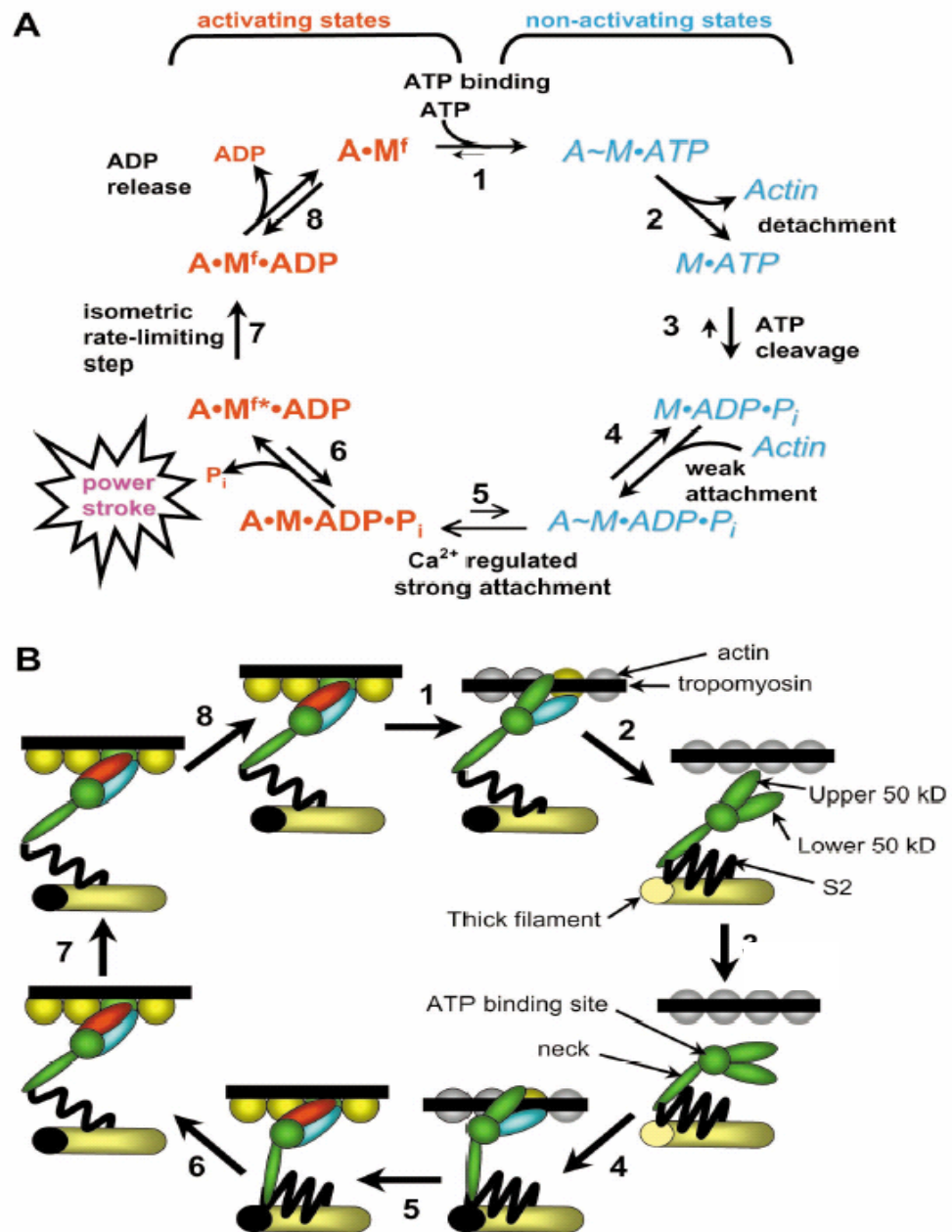


Figure 8. Cross-Bridge cycle kinetics.

(A) shows the cross-bridge cycle in terms of biochemical changes and the corresponding structural changes are shown in (B) (Gordon et al. 2001)

1.2.3.3 Myosin heavy chains (MHC)

In the human heart two sarcomeric myosin II genes are expressed generating two isoenzymes of the myosin heavy chain (designated α and β -MHC). These are located in tandem on the long arm of human chromosome 14q11.2-q13 (Saez et al. 1987). In the normal heart both MHC isoenzymes are expressed in a tissue-specific manner: the α -MHC is preferentially expressed in the atrium, and the β -MHC is almost exclusively expressed in the ventricle (Bouvagnet et al. 1984).

The human α -MHC contains 1939 amino acids residues (Matsuoka et al. 1991) while the β -MHC contains 1935 amino acids (Jaenicke et al. 1990). A total of 131 residues differ between both heavy chains and most of these differences are confined to regions of biological significance in the S1 subfragment such as the N-terminus, the ATP binding pocket, the actin binding cleft, the light chain binding domain and in the two hinge regions further down in the rod (tail) domain (Schaub et al. 1998).

In the hypertrophied atrium considerable amounts of β -MHC are expressed (Gorza et al. 1984; Mercadier et al. 1983), which is associated with a decrease in maximal shortening velocity (Arndt et al. 1989). α -MHC, however, is either found to be a minor component of human ventricular myosin (Gorza et al. 1984; Hirzel et al. 1985; Mercadier et al. 1983) or could not be detected at all (Ritter et al. 1999). Furthermore, there are no changes in α -MHC expression during hypertrophy of the human ventricle (Gorza et al. 1984; Hirzel et al. 1985; Mercadier et al. 1983; Ritter et al. 1999).

1.2.3.4 Myosin light chains (MLC)

Two types of myosin light chains (MLC), essential and regulatory, are associated with the neck region of the MHC. The essential MLC is designated as the MLC-1 or alkali MLC. The regulatory MLC is designated as MLC-2 or phosphorylatable MLC or 5,5-dithio-bis-(2-nitrobenzoate)-MLC (Ritter et al. 1999). Together with calmodulin and troponin C, both types belong to the superfamily of EF hand Ca^{2+} binding proteins (Moncrief et al. 1990).

In the human heart two different genes encode the essential myosin light chain isoforms, the ventricular-specific (VLC-1) and an atrial specific (ALC-1). VLC-1 is located on chromosome 3p21 (Fodor et al. 1989), coding for a 194 amino acid protein, which is the same isoform as the MLC-1 present in the adult slow skeletal muscle. ALC-1 is located on chromosome 17q21 (Seharaseyon et al. 1990) coding a 196 amino acid protein. Several MLC-2 isoforms exist in the human, preferentially expressed in the atrium (ALC-2) or in the ventricle (VLC-2). VLC-2 has been mapped to chromosome 12q23-q24 (Macera et al. 1992) in human encoding a 166 amino acid protein. ALC-2 is composed of 175 amino acids (Hailstones et al. 1992), but no data are available yet about the chromosomal localization. Electrophoretic analysis suggests the existence of two different VLC-2 isoforms in the human heart having the same molecular weight but different isoelectric points (VLC-2a for the more acidic and VLC-2b for the more basic isoform) (Price et al. 1980).

In the normal human heart mainly the VLC-2b isoform is expressed (LC-2b to LC-2a ratio of 2.3) (Morano et al. 1997; Morano et al. 1996). In most patients with limited cardiac functions, this ratio remains at its normal level. However, recently it was found that in patients with HOCM VLC-2a expression declines in favor of the VLC-2b form (Ritter et al. 1999).

Expression of ALC-1 is tissue specific and developmentally regulated. Human embryos express large amounts of ALC-1 both in the whole heart and in skeletal muscle (Barton et al. 1985). ALC-1 protein levels decrease in the ventricle to undetectable levels during early postnatal development but persisted in the atrium throughout the whole life (Fallot 1963).

The situation differs in patients with congenital heart disease such as Tetralogy of Fallot. Tetralogy of Fallot is a complex congenital heart disease characterized by four components: right ventricular infundibular stenosis, ventricular septal defect, dextroposed aorta overriding the interventricular septal defect, and right ventricular hypertrophy (Auckland et al. 1986). The hypertrophied right ventricle of children with tetralogy of Fallot express large amounts of VLC-1 in the atrium (Shi et al. 1991) and ALC-1 in the ventricle, up to adulthood (Auckland et al. 1986). Similarly, the hypertrophied left ventricle of patients with ischemic, dilative, and hypertrophic

cardiomyopathy express ALC-1 (Morano et al. 1997; Ritter et al. 1999; Schaub et al. 1998). Surgical intervention and subsequent normalization of the hemodynamic state decrease ALC-1 expression in these patients (Sutsch et al. 1992).

MLC-1 binds not only to the neck domain of the MHC (Rayment et al. 1993) but also with its N-terminus to the C-terminus domain of actin (Hayashibara et al. 1994; Morano et al. 1997; Sutsch et al. 1992; Trayer et al. 1987). Thus MLC-1 tethers the MHC to the actin filament. It has been demonstrated that MHC and MLC-1 bind to different actin monomers (Timson et al. 1998). Binding of MLC-1 to actin cannot be predicted from the crystal structure of myosin S1 (Rayment et al. 1993). This is due to the limited resolution of the three-dimensional structure of the N-terminus of MLC-1 (Rayment et al. 1993). In fact, around 40 N-terminal amino acid residues of MLC-1 are not seen in the crystal structure (Rayment et al. 1993). This missing part of MLC-1 contains ten Pro and ten Ala residues, which could form an antenna-like structure long enough to bridge the gap to the actin filament (Morano 1999).

Experimental evidence for the functional importance of the MHC/actin tether has been obtained by weakening the tether on the MLC-1/actin interface and/or MLC-1/MHC interface and simultaneous registration of cross-bridge function. Inhibition of the MLC-1/actin interaction by peptide competition using synthetic N-terminal MLC-1 peptides increases force production and shortening velocity of both demembrated (skinned) and of intact electrically driven human ventricular fibers (Morano et al. 1995) as well as myofibrillar ATPase activity (Rarick et al. 1996).

Assuming that tethering MHC to the actin filament via MLC-1 imposes a load on the myosin cross-bridge, thus relieving or weakening the MHC/actin tether decreases this load and accelerates cross-bridge cycling kinetics and at the same time enhances tension output per cross-bridge, thus increasing contractility (Morano et al. 1995).

The ALC-1 and VLC-1 differ in the primary structure of the N-terminus (Fodor et al. 1989). Indeed, the affinity for actin of the N-terminal peptide 5–14 derived from ALC-1 is significantly lower than the actin affinity of the corresponding N-terminal peptide of VLC-1 (Morano et al. 1997). These results support the idea that binding of ALC-1 to actin is weaker than the binding of VLC-1 to actin, representing a weaker MHC/actin tether

(Morano et al. 1996): because of its low actin affinity ALC-1 is a weaker MHC/actin tether than VLC-1 and has increased cross-bridge cycling kinetics and force generation.

1.2.3.5 Regulation of ALC-1 expression in the heart

Regulation of ALC-1 expression in the human heart is still not well understood. In the mouse two E boxes, which interact with muscle-specific basic helix-loop-helix (bHLH) regulatory proteins of the MyoD family, and a diverged CArG box, which binds to the serum response factor, exist within the first 630 bp of the ALC-1 promoter region (Catala et al. 1995).

E boxes have been shown to be sufficient for ALC-1 transcription regulation during skeletal muscle differentiation (Catala et al. 1995). bHLH regulatory factors of the MyoD family regulate skeletal muscle differentiation by forming heterodimers with E12 bHLH factors that bind to E-box elements, thus increasing the transcription rate of target genes (Olson 1992). Recently two cardiac-specific bHLH proteins homologous to the MyoD family have been detected in the heart, designated as the E and D forms of heart–autonomic nervous system–neural crest derivative (HAND) (Cserjesi et al. 1995; Srivastava et al. 1995). They are important for early development and looping of the embryonic heart (Srivastava et al. 1997). Since both HAND transcription factors bind weakly to E-box as E12 heterodimers, the ALC-1 may be a target gene. Recently it has been reported that in the human hypertrophied ventricle there is upregulation of HAND gene expression and a positive correlation between HAND and ALC-1 mRNA (Ritter et al. 1999). Furthermore, ALC-1 expression may be regulated by endogenous antisense ALC-1 mRNA present in the human ventricle (Ritter et al. 1999). Moreover Ca^{2+} -calmodulin-dependent processes, which are involved in the development of human heart hypertrophy, increased the activity of the human ALC-1 promoter. Both activation of calcineurin (CaN) and Calmodulin dependant kinase IV (CaMKIV) revealed a potent role in human ALC-1 gene regulation (Woischwill et al. 2004).

1.2.3.6 Functions of ALC-1 in the heart

Skinned fiber studies showed that the shortening velocity, rate of tension development, isometric force generation, and Ca^{2+} sensitivity of isometric force generation increase upon partial replacement of VLC-1 by ALC-1 in the human ventricles (Morano et al. 1997; Morano et al. 1996). Furthermore, there was a significant positive correlation between ALC-1 expression and $\text{dP/dt}_{\text{max}}$ of patients with hypertrophic obstructive cardiomyopathy (HOCM) in vivo (Ritter et al. 1999). Thus crossbridge cycling kinetics and tension generation per cross-bridge are modulated by differential expression of MLC-1 genes. These results demonstrated for the first time that there is a molecular mechanism which allows the ventricular cardiomyocyte to adjust to enhanced work load through modification of the structure of the molecular motor – the partial substitution of VLC-1 by ALC-1 which increases power output of the sarcomeric motor macromolecules and improves cardiac contractility (Morano 1999). These results have been supported in a transgenic mouse model overexpressing the mouse ALC-1. By the examination of the chemically skinned fibre function, the ventricular fibres from the transgenic mice had a higher V_{max} of shortening when compared to non-transgenic mice. Furthermore this light chain Isoform switch in the transgenic mouse model lead to increased contractile functions at the whole heart level (Fewell et al. 1998).

1.3 Aim of the study

The functional properties of the human atrial essential myosin light chain (hALC-1) has never been evaluated in an intact heart preparation on the whole organ level. Functional examination of the chemically skinned ventricular fibers from a transgenic mouse model overexpressing the mouse ALC-1 showed a higher maximal shortening velocity (V_{max}) when compared to non-transgenic mice: In the mouse heart, 95% replacement of mouse VLC-1 by the mouse ALC-1 was accompanied by a 1.78-fold increase in V_{max} of shortening. However chemically skinned ventricular fibers of patients expressing the hALC-1 with 20% replacement of human VLC-1 by human ALC-1 showed 1.88-fold increase in maximal shortening velocity (V_{max}). Although the data are consistent, it appears that the effect of mouse ALC-1 is attenuated as compared with hALC-1. These data suggest that there is a significant difference between the human and mouse ALC-1 isoforms at the functional level. To verify the functional efficiency of hALC-1 compared with mouse ALC-1 and to analyze hALC-1 functions in intact whole heart preparations, a transgenic rat-model overexpressing the hALC-1 was produced and characterized at the protein and functional levels.

2 Materials

2.1 Equipments

Amersham Pharmacia Biotech, Amersham place, England

Nitrocellulose membrane, hybond ECL

YT Recorder REC 111

MALDI-TOF software for Mass spectrometry

Biometra, Gottingen, Germany

PCR-Cycler

Bio-Rad, Munich

Bio-Rad Trans-blot SD, semi-dry transfer cell

BIOTEC-FISCHER, Reiskirchen, Germany

Light box

Calibrated imaging densitometry, California, USA

BIO-RAD GS-710

Definiens, Munich, Germany

Proteome Weaver software analysis program

Eppendorf, Hamburg, Germany

Thermo-shaker

Hugo-Sachs Electronic (Germany)

Software HEM Notocord

The Landgendorff-perfusion apparatus

Kodak, Rochester, NY

X ray films

Shimadzu Corporation, Kyoto Japan

Spectrophotometer UV-1201

Zeiss, Jena

Axioplan fluorescence microscope

MC 100 automatic camera

2.2 Chemicals

Amersham Pharmacia Biotech, Amersham place, England

Chemiluminescence's reaction Kit

BstYI- restriction enzyme

Hind III- restriction enzyme

XbaI- restriction enzyme

Biogenes, Berlin, Germany

Anti-rabbit antibody

Bio-Rad, Munich

Tween 20

PBS

Diagnostic Chemicals Limited

isopropyl (-D)-thiogalactopyranoside

Invitrogen GmbH, Karlsruhe, Germany

BL21 (DE3) pLysS cells

Expression vector pRSETA

PCR-Kit

Merck, Darmstadt, Germany.

DNase

HCl

K_2HPO_4

KH_2PO_4

$MgSO_4$

$NaHCO_3$

Na-K tartrat

$Na_4P_2O_7$

$NaPO_4$

Molecular Biochemicals Roche, Mannheim, Germany

Protease inhibitor mixture

proteinase K

Molecular Probes, Inc. USA

Secondary anti-mouse antibodies

Secondary anti-rabbit antibodies

Qiagen, Germany

NiNTA-agarose beads

Reanal-Budapest Hungary

Temed (N, N, N, N, tetramethylethylene diamine)

Roth Karlsruhe

APS (ammonium peroxodisulfate)

EDTA

KCl

Methanol

NaCl

Na₂CO₃

Sodium lauryl sulfate (SDS)

Serva, Heidelberg, Germany

Acrylamid

Ampholyte mixture Servalyte

BSA (bovine serum albumin)

CaCl₂

Coomassie blue R-256

DTT (dithiothreitol)

Glucose

Glycerol

Glycine

Ponceau S

Sucrose

Sodium dodecylsulfate (SDS)

Tris

Sigma Chemical Co., St. Louis, MO

Albumin

β -mercaptoethanol

Bromophenol blue

Chloral hydrate

CuSO_4

Folin

Isopropanol

MgCl_2

Monoclonal antibody against α -actinin

NaN_3

Paraform aldehyde

Pepstatin A

RNAse A

Thiourea

Urea

3 Methods

3.1 Transgene construction and generation of transgenic rats

For generation of the transgene construct, a full-length human ALC-1 (hALC-1) cDNA (Hemp4; -82-+768) was kindly provided by A. Starzinski-Powitz, Frankfurt, Germany (Zimmermann et al. 1990) and cloned downstream of the rat alpha-myosin heavy chain promoter (Hoffmann et al. 2001), followed by the polyadenylation signal of SV40 (Fig. 9).

The final 2.45-kb transgene construct was linearized with XbaI, purified by agarose gel electrophoresis, and used to generate transgenic rats as described (Popova et al. 2002) with the exception that oocytes from inbred (WKY) rats were used for pronuclear microinjection (Popova et al. 2002)..

3.2 Genotyping of the genomic DNA from the transgenic-rat tails.

The tails were overnight incubated in Tail Buffer (5mM Tris/HCL buffer, 100mM EDTA, 100mM NaCl & 1% SDS) & Proteinase K, placed in a thermo-shaker (Eppendorf, Hamburg) at 55c°.

The genomic DNA was extracted using 5M NaCl solution, RNase A and isopropanol for pellet precipitation. The pellet was then washed with 70% ethanol and left for air-drying. The pellet was dissolved in 100µl 1xTE buffer (10mM Tris/HCL, 1mM EDTA in sterile water) with OD spectrophotometric measurement, the DNA concentration was estimated (UV-1201 spectrophotometer, Shimadzu Corporation, Kyoto Japan).

The presence of the transgene in genomic DNA from tail biopsies was verified by PCR in a reaction volume 50µl using 20 ng from each tail sample, distilled H₂O in addition to the PCR kit (50 mM MgCl₂, 10x buffer without MgCl₂, 10 Mm dNTP-Mix and Taq polymerase) (Invitrogen, Karlsruhe, Germany) in addition to the two primers: GCCAAGGGATCAAAGGAGGA and TTGGCTGCCTCCTTCTTAGG, which were

specific for the transgene and amplified a 606 bp fragment. The reaction was run for 28 cycles in the PCR-Cycler (Biometra T-Gradient).

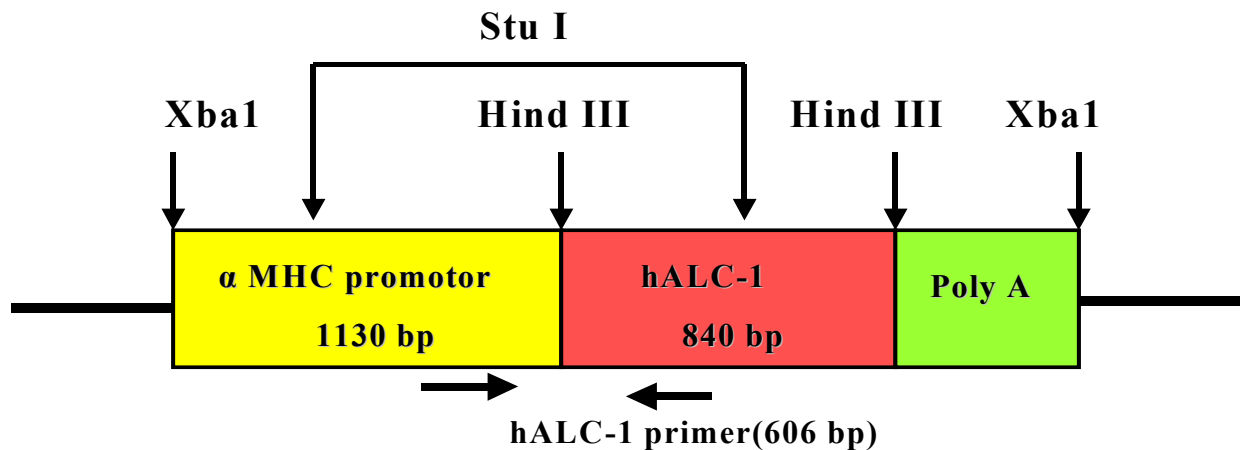


Figure 9. Schematic representation of the construct used to generate the transgenic rats.

The hALC-1 cDNA is linked to the α -MHC promoter followed by the polyadenylation signal of SV40. Relevant restriction sites are represented on the diagram. The final transgene construct was linearized with XbaI, purified by agarose gel electrophoresis and used to generate transgenic rats. Arrows indicate primers used for genotyping of the transgenic rats by PCR.

3.3 Generation of the hALC-1 specific antibody

The anti-hALC-1 antibody was raised in New Zealand White rabbits against the synthetic peptide (PAPEAPKEPAFDPKS) according to a standard protocol (Haase et al. 1993). The antigenic epitope comprised the amino acids 29–43 of hALC-1: an epitope in which hALC-1 (Acc. No. P12829) and rat ALC-1 (Acc. No. P17209) share only 2 out of 15 amino acid residues.

The antibody-containing serum fractions were affinity purified on the peptide antigen column. The resulting affinity-purified antibody fraction was depleted of antibodies cross-reacting with rat cardiac proteins by incubation with acetone-treated rat cardiac tissue. A second round of affinity chromatography on the peptide antigen column recovered the human ALC-1 specific antibodies.

3.4 Recombinant human ALC-1

For cloning of the hALC-1 cDNA in a bacterial expression-system, the already established clone (Hemp4) was used (Fig. 9). An 812 bp BstYI-Hind III fragment carrying the complete protein-coding region of hALC-1 (594 nucleotides) was inserted into the BamH1-HindIII site of the expression vector pRSETA (Invitrogen, Karlsruhe, Germany) to yield hALC-1 as an N-terminally HIS-tagged fusion protein (hALC-1_{HIST}) construct.

Single colonies of BL21 (DE3) pLysS cells (Invitrogen, Karlsruhe, Germany) were transformed with the hALC-1_{HIST}. Protein expression was induced with 0.1 mM isopropyl (-D)-thiogalactopyranoside (Diagnostic Chemicals Limited) for 3-4 h at 37°C.

The cells were collected by centrifugation, resuspended and sonicated twice for 45s. The sonicated material was centrifuged and the supernatant was incubated with 1 ml of Ni-NTA-agarose beads (Qiagen, Germany). The beads were extensively washed and the hALC-1_{HIST} fusion protein was then eluted. The purified hALC-1_{HIST} had an apparent molecular mass of 35-kDa (see below).

3.5 Myosin purification.

Myosin was extracted and purified from the left ventricular tissues of TGR/hALC-1 and WKY rats. The ventricles were crashed in liquid nitrogen and extracted for 20 m at 4°C with 3.4 volumes (w/v) of a modified Guba-Straub solution (0.3M KCL, 0.1M NaPO₄, 1 mM MgCl₂, 10 mM Na₄P₂O₇, 10mM EDTA, 1% NaN₃ (w/v), 1% β-mercaptoethanol) pH 6.5.

The crude extract was used for purification of myosin as described (Offer et al. 1973) except that the actomyosin was dissociated in 150 mM Na₄P₂O₇, 6mM EDTA, 3mM DTT, and 9mM ATP at pH 7, before ammonium sulphate fractionation.

The myosin was dialysed overnight in 0.5 M NaCl, 0.01 M Tris and 1mM EDTA at pH 7. Myosin concentration was determined at 280nm using the specific absorption coefficient (1mg/ml=0.52).

3.6 Composition analysis of purified myosin and human atrial tissue

The protein composition of the human atrial tissues and the purified myosin of the transgenic and control rats (TGR/hALC-1, WKY) was analysed by SDS-polyacrylamide gel electrophoresis according to a modified laemmli gel method (Laemmli 1970). Mini-protean II dual slab cell (Biorad) was used which provides a gel with the following dimensions: 80 mm wide and 70 mm long and 1.5 mm thick. A 12 % separating gel (see table 1) was prepared and applied between the glass plates. The solution was covered with distilled water to provide a flat gel surface. After polymerisation, a 4% stacking gel (see table 1) was prepared and applied above the separating gel, after the water was poured off. A comb was placed into the stacking gel solution, and it was allowed to polymerise. After polymerisation, the comb was removed and each well was loaded with 70-µg proteins. The protein samples were diluted 1:3 with sample buffer (0.5 Tris-HCl, pH 6.8 12.5% (v/v); glycerol 10% (v/v); SDS 2% (w/v); 2-βmercaptoethanol 5% (v/v); bromophenol blue 0.001% (w/v)) and heated 5 minutes at 95 °C.

The gels were stained with coomassie blue R-256 and scanned to determine the relative content of myosin light chains. The same protein samples were also separated by SDS-polyacrylamide gel electrophoresis and then processed for Western blot analysis.

	Separating gel (12%)	Stacking gel (4%)
Acrylamid 30 %	4 ml	0.66 ml
0.75 M Tris-HCl, pH 8.8, 0.2% SDS	5 ml	—
0.25 M Tris-HCl, pH 6.8, 0.2% SDS	—	2.5 ml
Distilled water	0.78 ml	1.72
Temed 10%	70 μ l	50 μ l
APS 10%	140 μ l	100 μ l

Table 1. Recipes for separating and stacking polyacrylamide gels, based on the buffer system of Laemmli.

3.7 Quantification of transgene expression.

Rats were sacrificed, the hearts were removed, and the ventricles were immediately frozen in liquid nitrogen. The tissue was stored at -80°C until protein preparation. The total protein fraction was extracted from frozen tissue specimens (20-40 mg) by homogenization with a motor-driven glass-teflon homogenizer in SDS-sample buffer (5% SDS, 50 mM Tris-HCl, pH 7.5, 250 mM sucrose, 75 mM urea, 10 mM dithiothreitol), denatured for 3 min at 95°C , and cleared by centrifugation.

The supernatant containing the total SDS-extracted proteins was removed and the protein concentration was determined by a modified Lowry method using 10% SDS and the Lowry mixture (CuSO_4 , 2% NaK tartrat, 2% Na_2CO_3 (Wang et al. 1975) using bovine serum albumin as the standard.

Ventricular SDS-extracted proteins (80 μ g) and different concentrations of the hALC-1_{HIST} were separated by SDS-PAGE on a 12% resolving gel which was equilibrated for 10 minutes at room temperature in a transfer buffer (25 mM Tris base; 192 mM glycine and methanol 20% (v/v)). The proteins were electrophoretically transferred (Bio-Rad Trans-blot SD, semi-dry transfer cell) from the gel to nitrocellulose membrane (Hybond-C, Amersham) for 2 h at 250 mA. Following transfer, the membrane was incubated with Ponceau staining solution for 10 minutes at room temperature.

The nitrocellulose membrane was blocked with 15% ovalbumin (0.1% Tween; 20 mM Tris base and 137 mM NaCl). The transfers were incubated overnight with the affinity-purified anti-human ALC-1 antibody at a concentration of 0.5 μ g IgG/ml and subsequently with the secondary peroxidase-conjugated anti-rabbit antibody (Biogenes, Berlin, Germany) for 1 h at room temperature. Between each step, the membranes were washed by TBS (20 mM Tris base, 137 mM NaCl, pH 7.6) and TBST (20 mM Tris base, 137 mM NaCl and 0.1% Tween)

Immunoreactive proteins were visualized with the enhanced chemiluminescence's reaction Kit (ECL, Amersham) and X ray films (X-Omat, Kodak, Rochester, NY). The signals were scanned by densitometry using BIO-RAD GS-710 (calibrated imaging densitometry, California, USA).

3.8 Immunofluorescence microscopy.

For immunofluorescence detection of the hALC-1 in the ventricular tissues, animals were anaesthetized (30 mg/kg Chloral hydrate), the hearts were removed, and 1mm³ left ventricular tissue samples were taken from the hearts and fixed by incubation for 2 h at room temperature with 4% paraformaldehyde, 0.1M PBS and 0.18M sucrose.

The tissues were washed (3 times each for 5 m) with 0.1M PBS, then incubated overnight in 2.3M sucrose, 0.1M PBS, and subsequently frozen in liquid nitrogen. Tissue sections (1 μ m) were incubated with blocking buffer (20 mM Tris/HCL pH 8.4, 630mM NaCl, 0.05% Tween 20, 0.02% NaN₃, 1% BSA) for 30 m at room temperature.

Tissue sections were incubated with anti hALC-1 antibody (rabbit antibodies) and anti-MHC antibodies (mouse antibodies) for 2 h at 37°C (2µg/ml). In a different set of experiments, tissue sections were incubated with the anti hALC-1 antibody and a monoclonal antibody against α -actinin (Sigma, St. Louis, Mo).

The tissues were washed with the blocking buffer and incubated with secondary antibodies (Alexa 594, red) anti-rabbit antibodies (Alexa 488, green) anti-mouse antibodies (Molecular Probes, Inc. USA) (5µg/ml) for 1 h at 37 °C.

Fluorescence was detected using an axioplan fluorescence microscope with appropriate filter systems. Micrographs were followed with an MC100 automatic camera with Kodak Tmax 400 film.

3.9 Analysis of the ventricular proteome by 2D-PAGE.

3.9.1 Preparation of the protein samples:

Four TGR/hALC-1 and four WKY (12 weeks-old) rat ventricular tissues were used for 2D gel electrophoresis. Rat ventricular tissues in 2.2 parts v/w of 50 mM Tris buffer, pH 7.5, containing 50 mM KCL, 20 % v/v glycerol and 4 % w/v 3-[(3-chloramidopropyl) dimethylammonio-1-propanesulfonate (CHAPS)], were combined with protease inhibitor mixture [0.08 parts v/w of one Complete TM tablet (Molecular Biochemicals Roche, Mannheim, Germany), dissolved in 2 ml of 100 mM KCL, 20 % v/v glycerol and 50 mM Tris, pH 7.1. and 0.02 parts of 1 mM PMSF (phenylmethylsulfonylflouride) together with 1.4µM pepstatin A dissolved in ethanol].

All components were ground to a fine powder in a motor placed in liquid nitrogen bath. Sonication was performed in a water bath by adding 0.034 parts of glass beads to the defrosted homogenate. The resulting extract was stirred for 30 min at 4⁰ C in the presence of 0.023 parts v/w of 50 mM Tris buffer, pH 7.5, containing 50 mM KCL, 20 % v/v glycerol, 5 mM MgCl₂ x 6 H₂O and 0.025 parts v/w of DNase (Benzonase; Merck, Darmstadt, Germany).

Urea (6.5 M) and 2 M thiourea were dissolved in the sample. After dissolving, 0.01 parts v/w 70 mM DTT and 0.01 parts v/w ampholyte mixture Servalyte 2-4 (Serva, Heidelberg, Germany) were added and the homogenates were stirred for 30 min at 4° C. The samples were stored at – 80° C.

3.9.2 2D electrophoresis:

Protein extracts were purified by large-gel 2D (Klose 1999). The gel format was 46.4 cm (isoelectric focusing, pH range 3 -10) × 30 cm (SDS-PAGE direction) × 0.75 mm. Exactly 6 µl (containing 120 µg protein) of total protein extract were loaded on an isoelectric focusing tube gel (0.9 mm diameter).

3.9.3 Silver staining, spot detection and mass spectrometry

The proteins spots were visualized by an acidic silver staining procedure (Klose et al. 1995). The 2D silver-stained gels were analyzed visually on a light box (BIOTEC-FISCHER, Reiskirchen, Germany).

The total spot number of the protein expression-pattern was evaluated in both animal groups by using an automated software analysis program [Proteome Weaver imaging software 2.1.1 (Definiens)].

Mass spectrometry (MALDI TOF) was used for protein identification, 20 µl of each sample was loaded on 1.5 mm tube gels and stained with mass spectrometry compatible silver staining (Shevchenko et al. 1996).

3.10 Isolated perfused hearts (Langendorff method)

Animal experiments were performed using 12, 24 and 36 weeks-old transgenic (TGR/hALC-1) rats and age-matched wild type WKY rats. The rats were kept on a 12h light-dark cycle with 55% humidity at an ambient temperature of $23\pm 2^{\circ}\text{C}$ and given food, tap water and libitum. The institutional animal care body in the state of Berlin, Germany approved the studies.

For the Langendorff heart preparations (Langendorff 1895), hearts were excised from anaesthetized (30 mg/kg Chloral hydrate) and heparinized (500 U/kg) male transgenic and WKY rats after thoracotomy and then cannulated for retrograde aortic perfusion with a modified Krebs-Henseleit solution containing NaCl (118 mM), KCl (4.7mM), CaCl_2 (1.5mM), MgSO_4 (1.2Mm), NaHCO_3 (25 mM), Na_2EDTA (0.05 mM), KH_2PO_4 , (0.23 mM), 2.5% albumin and glucose (11.1 mM). The solution was saturated with 95% O_2 / 5% CO_2 pH 7.4.

The perfusion apparatus was from Hugo-Sachs Electronic (Germany). Systolic pressure was measured with a latex balloon, filled with ethanol/ H_2O , which was inserted into the left ventricle through the left atrium via a catheter to a (Isotec) transducer. The pressure in the balloon was set from 14–18 mmHg. The stimulation frequency was fixed at 340 beats/min. The perfusion was carried out at 37°C with a constant aortic pressure of 70 mmHg. Signals were recorded on a linear-corder mark 8 WR 3500. Contractile data were monitored and recorded by computer software (HEM, Notocord, France).

The recorded functional parameters were coronary flow, perfusion pressure, developed left ventricular pressure (LVP), maximal rate of pressure increase (+dP/dtmax) and maximal rate of pressure decrease (-dP/dtmax).

3.11 Statistical analysis

Values are expressed as mean \pm SEM. Analysis of significance was performed with the unpaired Student's t- test.

4 Results

4.1 Generation and basic characterization of the transgenic rats

The construct shown in Figure 9 was used to generate transgenic rats of the inbred WKY strain. The presence of the hALC-1 transgene in the genome was verified by a specific PCR protocol (Fig. 10) and Southern blot using DNA isolated from the tails of the animals. To the best of my knowledge this is the first transgenic rat model made on an inbred WKY background. Transgenic animals were morphologically normal. In particular, the heart weight/body weight ratio was not significantly different between TGR/hALC-1 and WKY control rats (Fig.11) indicating that the hALC-1 gene did not induce hypertrophic alterations in the heart of the transgenic animals.

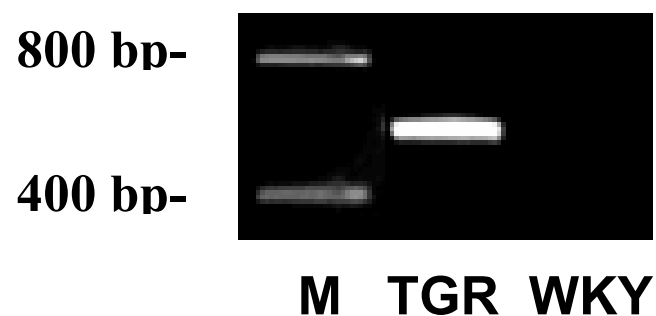


Figure 10. Genotyping of transgenic rats.

Genomic DNA from tail biopsies of a TGR/hALC-1 (TGR) and a control (WKY) rat was analyzed by transgene-specific PCR yielding a fragment of 606 bp only in TGR/hALC-1.

Heart weight/ body weight relationship

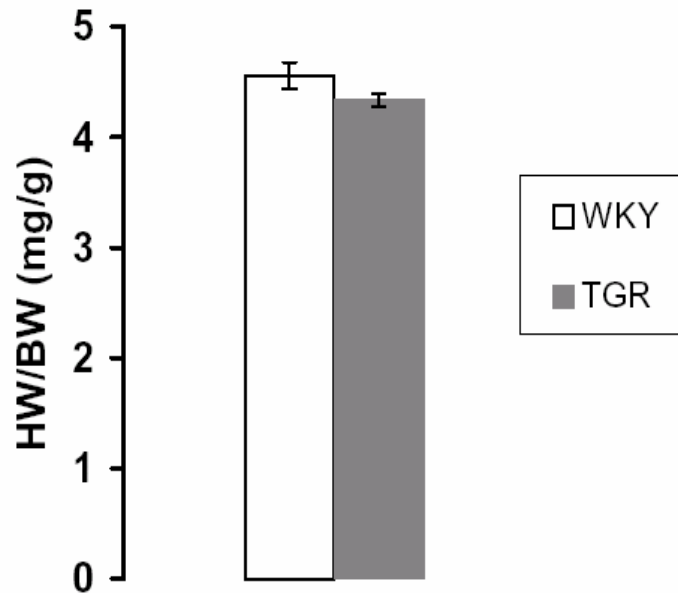


Figure 11. Heart weight/body weight relationship (HW/BW).

The heart weight/body weight relationship was evaluated in 12 weeks-old TGR/hALC-1 (TGR) and WKY animals. Revealing no significant difference between both groups. Values were expressed as means \pm SEM (n=7).

4.2 Quantification of the expressed hALC-1

To determine transgene expression at the protein level, a unique peptide antibody against human ALC-1 sequence was developed. Figure 13 illustrates a typical immunoblot analysis of the total protein fractions extracted from the ventricles of WKY or TGR/hALC-1 rats. The anti-human ALC-1 antibody specifically recognized a 28-kDa protein in the TGR/hALC-1 animals, i.e. the expected molecular mass of the human ALC-1. This apparent molecular mass is consistent with the migration of the immunostained ALC-1 in human atrial tissue extracts (Fig. 14B). The antibody did not cross-react with the ventricular light chains of WKY rats or any other proteins on Western blots of total rat ventricular proteins (Fig. 14B).

Recombinant HIS-tagged hALC-1 migrating at 35 kDa was used as standard to quantify the amount of expressed hALC-1 by Western blot analysis (Fig.12A). There was a linear relationship between the optical density of ECL-signals and recombinant h-ALC-1 which was used as standard curve (Fig. 12B).

Densitometric analysis of proteins extracted from 12-week old rats revealed an average amount of $17 \pm 4\mu\text{g}$ hALC-1 per mg of SDS-extracted ventricular proteins (n=7). Assuming myosin represents 45% of the whole SDS-soluble protein and the MLC-1 is 10% of the whole myosin (Swynghedauw 1986), therefore the expressed hALC-1 represents 37% of whole MLC-1. Moreover an age-dependent decline in transgene expression was observed in the same animal line.

By quantifying hALC-1 expression in 24 and 36-week old TGR/hALC-1, the average amount of hALC-1 expression in the 24 weeks-old rats declined significantly ($p < 0.05$) to $9.5 \pm 3\mu\text{g}$ hALC-1 per mg of whole SDS-soluble protein (n=8), which represents 21% of the whole MLC-1. In the 36-week old TGR/hALC-1 rats, hALC-1 expression was significantly reduced to $4.8 \pm 2\mu\text{g}$ hALC-1 per mg of whole SDS-soluble protein (n=10), which represents about 10% of the total MLC-1.

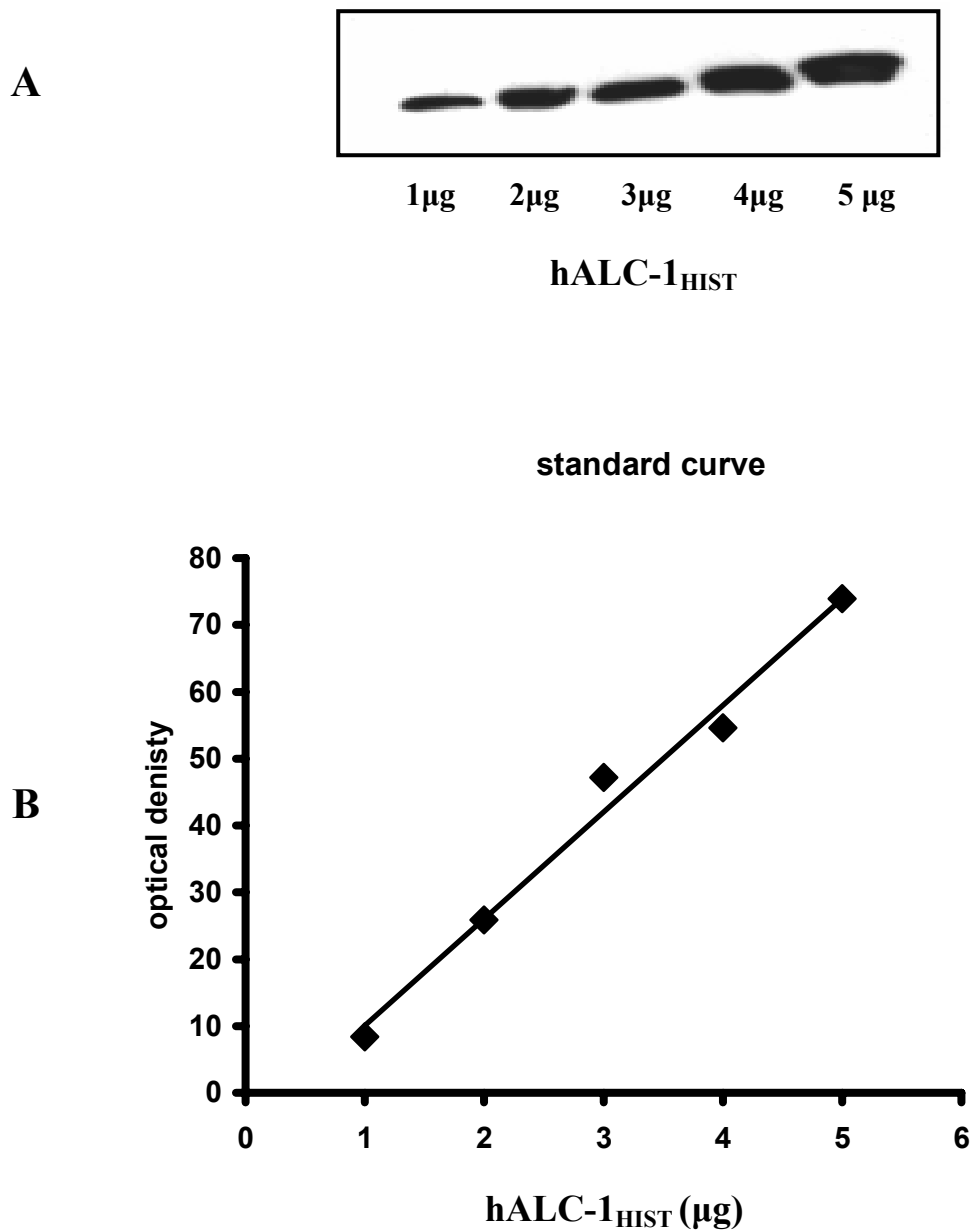


Figure 12. hALC-1_{HIST} Standard Curve .

(A) Different concentrations (1 μ g, 2 μ g, 3 μ g, 4 μ g & 5 μ g) of the hALC-1_{HIST} were identified by 12% SDS gel and Western Blot using anti human ALC-1 antibodies.

(B) The hALC-1_{HIST} signals were scanned densitometrically then plotted against the concentration for obtaining a standard curve for the estimation of protein content expressed by the transgene.

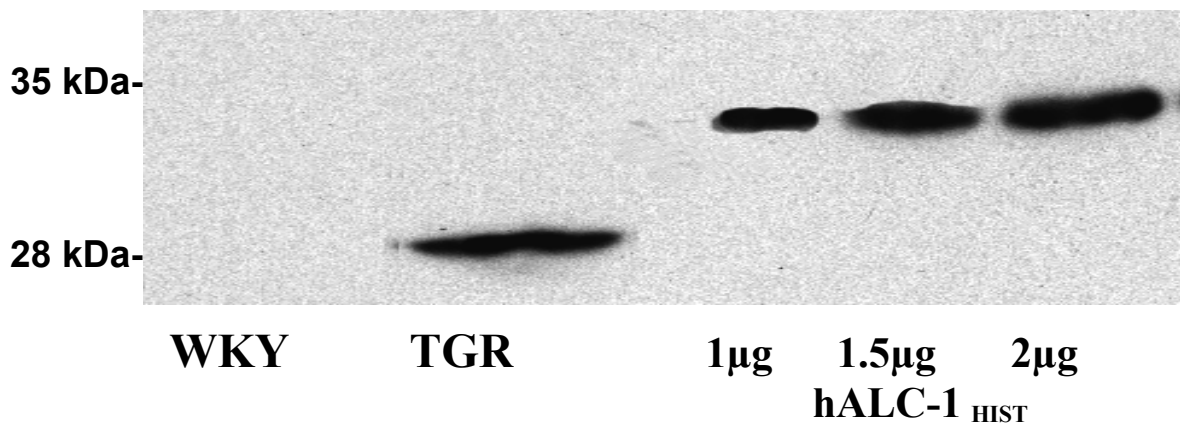


Figure 13. Quantification of the expressed hALC-1.

Immunoblot analysis of the total protein fractions (80μg) extracted from the ventricles of WKY or TGR/hALC-1 . The anti-human ALC-1 antibody recognized specifically the hALC-1 (28-kDa) protein in the TGR/hALC-1 animals. The antibody did not cross-react with the ventricular light chains of WKY rats. Recombinant HIS-tagged hALC-1 migrating at 35 kDa was used as standard (1, 1.5 and 2μg) to quantify the amount of expressed hALC-1.

4.3 MLC analysis

Figure 14A illustrates an SDS-PAGE gel for the separation of human atrial tissue SDS-extract (hAT) and left ventricular purified myosin preparations of TGR/hALC-1 and WKY animals, with assessment of the stoichiometry of the total MLC-1 isoforms (28 kDa) versus total MLC-2 isoforms (18kDa).

The bands were scanned densitometrically and the MLC-1/MLC-2 ratio was 1.2 ± 0.1 (n= 4) and 1.3 ± 0.03 (n= 4) respectively in the transgenic and WKY rats, showing no difference in MLC pattern in both animal groups.

Native hALC-1 (from human atrial tissue SDS-extract) as well as the rat VLC-1 co-migrated in SDS-PAGE (28 kDa) (Fig. 14A).

The anti-human ALC-1 antibody recognized specifically the hALC-1 in the myosin preparations of all TGR/hALC-1 animals (TGR/hALC-1) and the native hALC-1 in the human atrial tissue extract on immunoblot analysis (Fig. 14B) of human atrial tissue extract and left ventricular purified myosin preparations of TGR/hALC-1 and WKY rats. The TGR/hALC-1 revealed an identical molecular weight (28 kDa) to the native hALC-1.

To estimate the amount of replacement of the rat-endogenous VLC-1 by the hALC-1 left ventricular purified myosin preparations (20 μ g) of TGR/hALC-1 and WKY rat were separated by SDS-PAGE on a 12% resolving gel and transferred to a nitrocellulose membrane in a typical immunoblot analysis. hALC-1_{HIST} was used as standard to quantify the amount of expressed hALC-1 in the myosin preparations. The amount of hALC-1 associated with the purified TGR/hALC-1 myosin represented $20 \pm 2\%$ (n=4) of whole transgenic rat MLC-1.

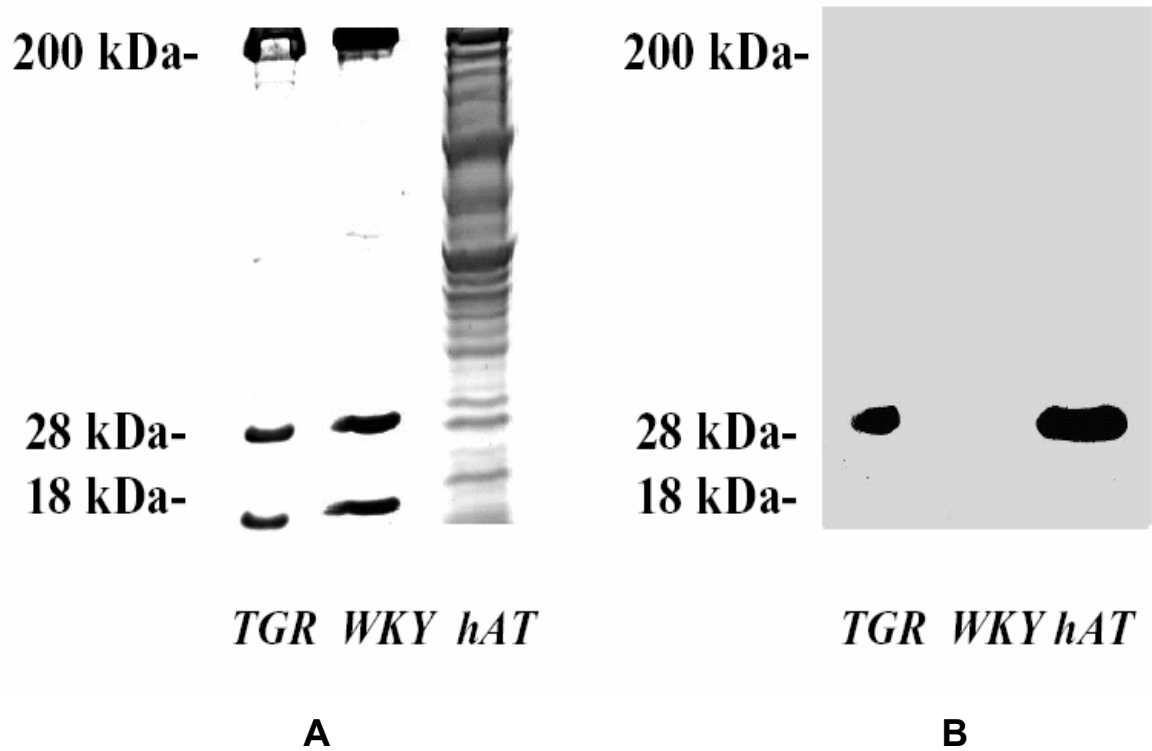


Figure 14. MLC composition analysis.

(A) SDS-Page for the purified myosin of a TGR/hALC-1 (TGR), WKY rats and human atrial tissue SDS-extract (hAT). Note the co-migration of the native hALC-1 (of the human atrial tissue SDS-extract) (28 kDa) and the rat VLC-1 (28 kDa).

(B) Immunoblot analysis of the hAT and the purified myosin preparations of TGR/hALC-1 and WKY rats.

4.4 Immunofluorescence Microscopy

Ventricular tissue sections from the transgenic animals were analysed using specific anti-hALC-1 antibodies and anti α -actinin antibodies. TGR/hALC-1 were investigated by double-labelling immunofluorescence microscopy, Z-lines were identified by alpha-actinin specific fluorescence, showing regular striated pattern that is consistent with labelling of the sarcomere (Fig. 15A).

The specific fluorescence of hALC-1 (Fig. 15B) in the sarcomere could be localized between the Z-lines by overlaying the hALC-1 and α -actinin labelling patterns, (Fig.15C). These observations confirm the appropriate placement of the hALC-1 into the contractile machine.

Furthermore, by double-labelling analysis using anti hALC-1 (Fig. 16B) and anti-MHC antibodies (Fig. 16A), mosaic patterns of transgene expression in cardiomyocytes were observed. The specific hALC-1 fluorescence signals of cardiomyocytes revealed different signal intensities, ranging from strong signals to undetectable levels of hALC-1.

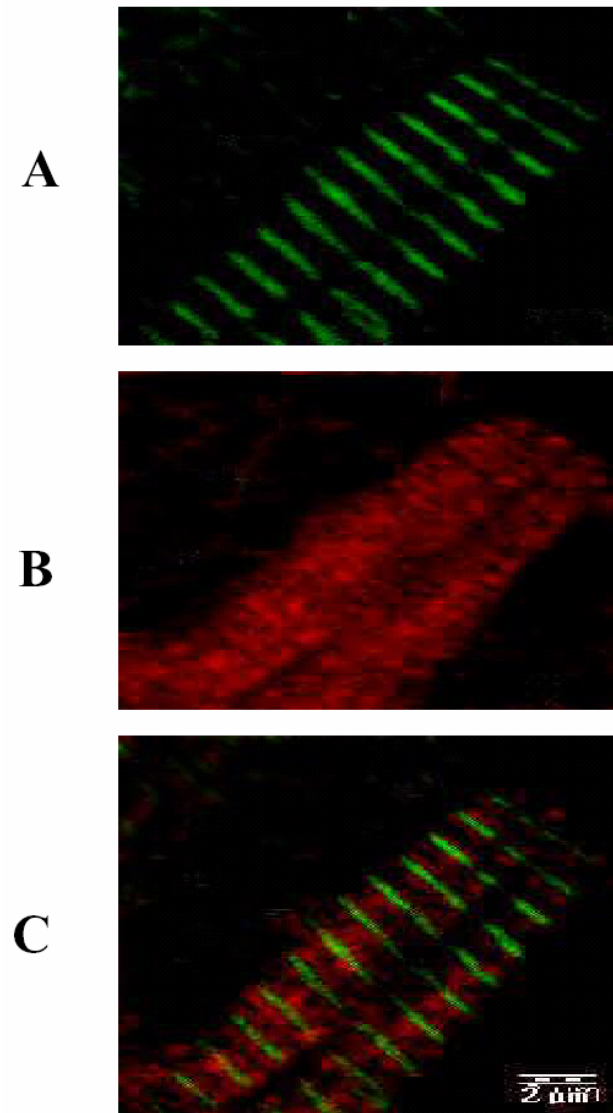


Figure 15. Immunofluorescence localization of the transgene-expression.

Left ventricular tissue sections from the transgenic animals were analysed by double-labelling immunofluorescent microscopy. α -actinin was detected by using anti α -actinin antibodies demonstrating its binding to the Z-bands with regular striated pattern that is consistent with labelling of the sarcomere (**A**). The hALC-1 in the ventricles of the TGR/hALC-1 was detected by using specific anti-hALC-1 antibodies (**B**). The hALC-1 and α -actinin labelling patterns were overlaid, showing the localization of the hALC-1 in-between the Z-bands of the sarcomere, (**C**).

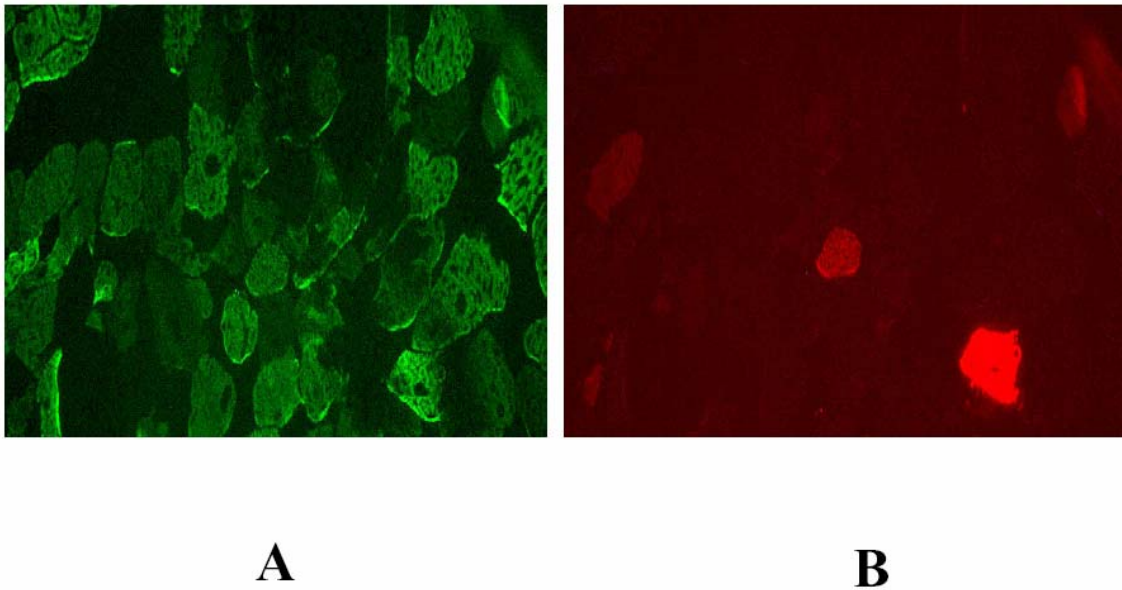


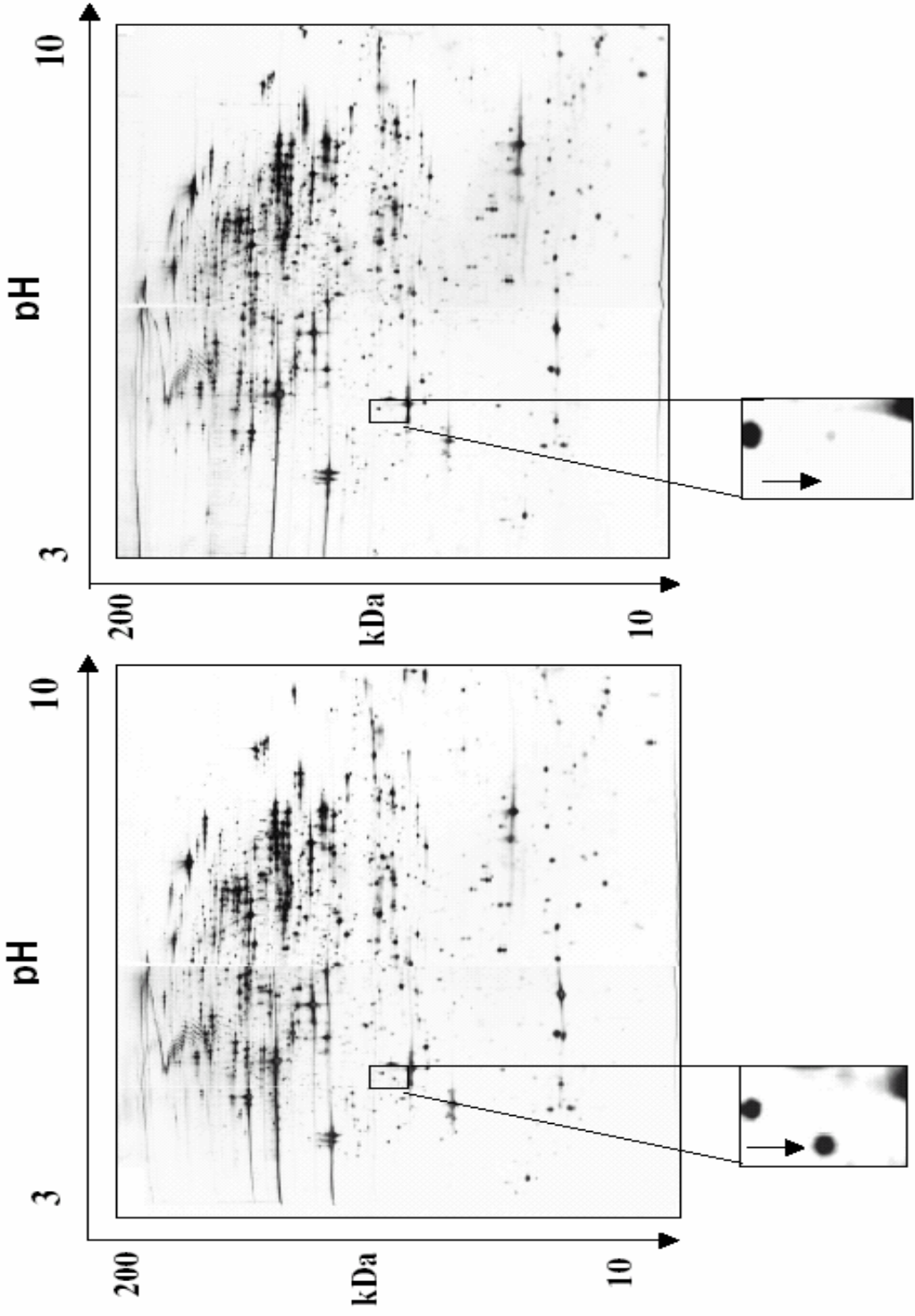
Figure 16. Expression-patterns of the transgene.

By double-labelling immunofluorescent analysis of the left ventricular tissue sections of the TGR/hALC-1, the tissues were incubated with anti-myosin heavy chain-antibodies demonstrating the myosin heavy chains (Green) **(A)**, and the anti-hALC-1 antibodies demonstrated the hALC-1 (Red) **(B)**. The specific hALC-1 fluorescence signals of cardiomyocytes revealed different signal intensities between very strong signals and undetectable levels of hALC-1.

4.5 Comparative proteome analysis

In a 2D-PAGE comparative analysis of the whole rat ventricular protein expression-patterns (4 pairs of 12 weeks-old TGR/hALC-1 and WKY rats), I was able to resolve approximately 3000 protein spots in each pattern.

The whole protein expression patterns in both animal groups showed no differences with the exception of the transgenic spot (Fig.17A and B) that was absent in all the WKY rats and present in all the TGR/hALC-1, but other spot variations existed in between the same animal group. The transgenic protein spot was identified by molecular weight and mass spectrometry and proved to be hALC-1.



B

A

Figure 17. Analysis of the ventricular proteome by 2D-PAGE.

Shown are the representative silver-stained gels of both animal groups at protein loads of 120 μ g. **(A)** Silver stained 2-D gel for 12-week old TGR/hALC-1 (pH 3 to 10) with a magnified section showing the transgenic hALC-1 protein spot (arrow). **(B)** Silver stained 2-D gel for 12-week old WKY rat (pH 3 to 10) with a magnified section showing the absence of the transgenic hALC-1 protein spot (arrow).

4.6 Functional properties of the transgene

Cardiac functions in the TGR/hALC-1 and WKY rats were evaluated by examining the isolated perfused hearts. Hearts were obtained from 12-24-36-week old animals.

Left ventricular functions were evaluated and there was a statistically significant improvement ($p < 0.001$) in the contractile functions of the 12-week old TGR/hALC-1 ($n=7$) compared to their age-matched control (WKY) ($n=7$) animals. This improvement is represented in an increase in: the developed left ventricular pressure (LVP) by 2.17-fold (Fig. 18), the maximum rate of pressure increase (contraction rate, $+dP/dt_{max}$) by 2.11-fold (Fig. 19) and the maximum rate of pressure decrease (relaxation rate, $-dP/dt_{max}$) by 1.91-fold (Fig. 20) in the TGR/hALC-1 compared to the age matched WKY rats.

While evaluating the contractile functions of the 24 and 36 weeks-old rats compared to the 12 weeks-old rats, there was an age-dependent decline of the improved contractility parameters tightly associated with a decline in transgene expression levels in the 24 and 36-week old TGR/hALC-1 ($n=8$ and 10-respectively) (Fig. 18, 19, 20).

In contrast, there was an age-dependent increase in contractility in the 24, 36 weeks-old WKY rats compared with 12 weeks old animals (Fig. 18 19, 20). Therefore, improved contractile functions of TGR/hALC-1 levelled-off to normal in 36 weeks-old animals.

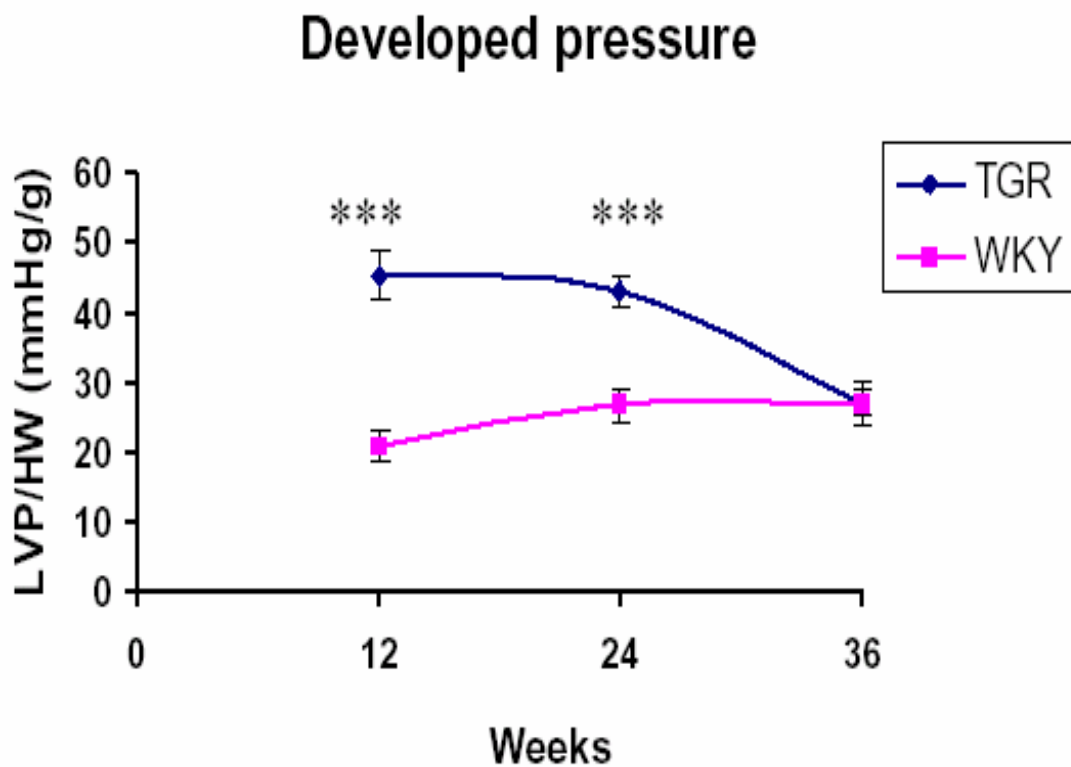


Figure 18. Developed left ventricular pressure (LVP):

Shown significant increase in the 12 and 24 weeks-old TGR/hALC-1 (TGR) compared to the age-matching WKY rats, while the 36 weeks-old rats showed no significant difference between the TGR/hALC-1 and WKY groups *** $p < 0.001$.

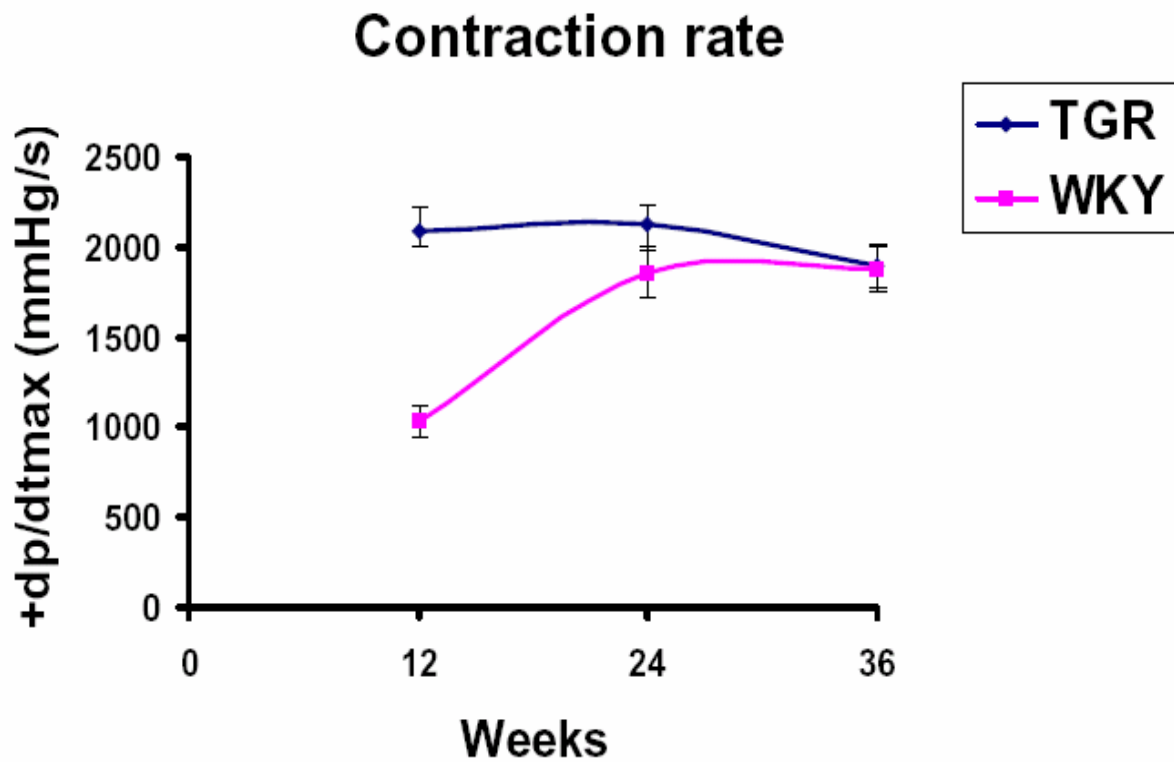


Figure 19. Maximum rate of pressure increase (+dP/dt max) (contraction rate): showed significant increase in the 12 weeks-old TGR/hALC-1 (TGR) compared to the age-matching WKY rats, while the 24 and 36 weeks-old rats showed no significant difference between the TGR/hALC-1 and WKY groups *** $p < 0.001$.

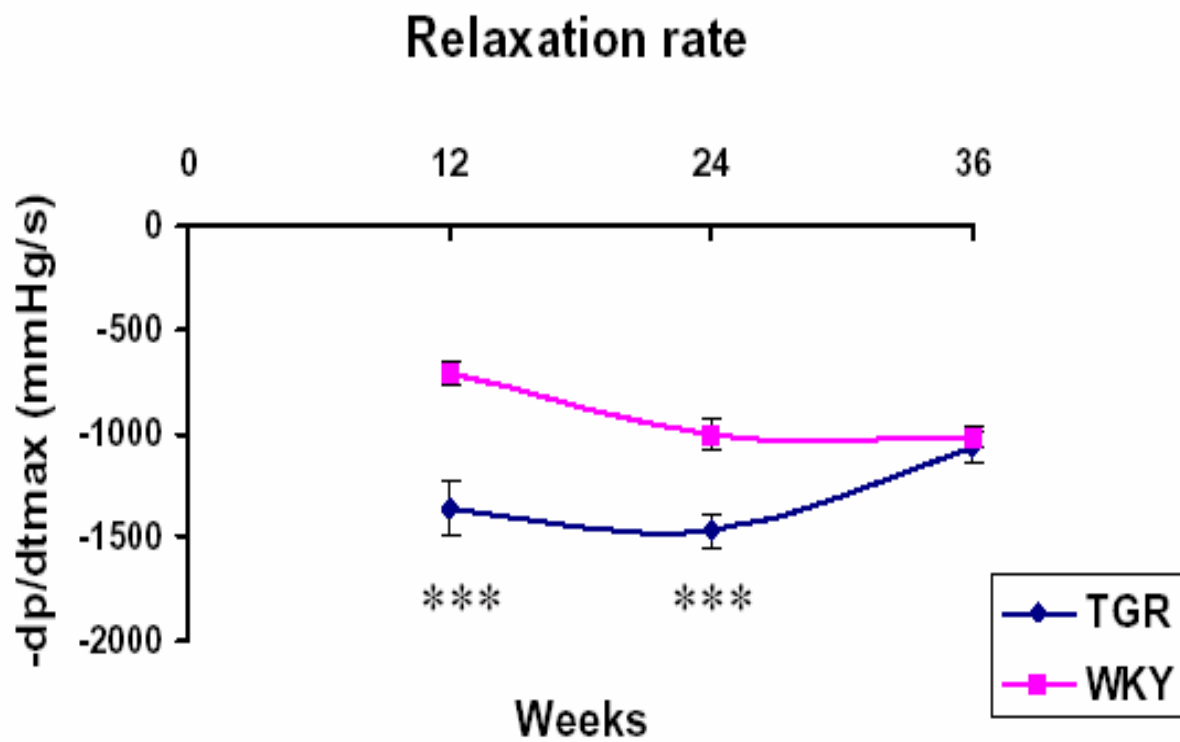


Figure 20. Maximum rate of pressure decrease (-dP/dt max) (relaxation rate): showed significant increase in the 12 and 24 weeks-old TGR/hALC-1 (TGR) compared to the age-matching WKY rats, while the 36 weeks-old rats showed no significant difference between the TGR/hALC-1 and WKY groups^{***} p<0.001.

5 Discussion

Myosin is a motor protein, which acts as the cross-bridge in the contractile apparatus of all muscle types. It interacts cyclically with the thin (actin) filament thus producing force and shortening while consuming ATP. Myosin cross-bridge action therefore represents an important process determining cardiac systolic and diastolic function (Lowey et al. 1971). Two types of myosin light chains (MLC), essential and regulatory, are associated with the neck region of the myosin heavy chains (MHC) (Moncrief et al. 1990).

Expression of the atrial-specific essential MLC (ALC-1) is tissue specific and developmentally regulated. ALC-1 is expressed in large amounts in the whole heart of human embryos (Barton et al. 1985), then is only restricted to the atrium in early postnatal development (Fallot 1963). The hALC-1 gene is located on chromosome 17q21b and encodes a protein of 196 amino acids (Seharaseyon et al. 1990). Regulation of cardiac contractility in the human ventricles by ALC-1 provided an alternative to the MHC regulatory mechanisms seen in a rodent-overloaded heart that responds by a MHC isoform shift from α -MHC (high ATPase activity) to β -MHC (low ATPase activity) (Morano et al. 1997; Morano et al. 1996; Sutsch et al. 1992). It was previously reported that human ventricular skinned fibers revealed an increase in maximal shortening velocity, rate of tension development, isometric force generation, and calcium sensitivity of isometric force generation upon partial replacement of VLC-1 by ALC-1 (Morano et al. 1997; Morano et al. 1996). Furthermore, there was a significant positive correlation between ALC-1 expression and dP/dt_{max} in patients with hypertrophic obstructive cardiomyopathy (HOCM) (Ritter et al. 1999).

The functional properties of the human atrial essential myosin light chain (hALC-1) has never been evaluated in an intact heart preparation at the whole organ level. Only correlations between the hALC-1 and hemodynamic data have been reported, such as systolic, end-diastolic pressure, end-diastolic volume index, mean pressure gradient and wall stress (Brodie et al. 1977; Grossman et al. 1972). Previous research has identified the beneficial functional effects of hALC-1 in-vitro cardiac preparations (human ventricular skinned fibers) of patients expressing hALC-1 (Morano et al. 1997; Morano et al. 1996; Ritter et al. 1999). Cardiac-specific overexpression of mouse ALC-1 was accomplished in transgenic mice. The changes at the motor protein and fiber levels

were translated into changes in the contractile function of the whole mouse heart, represented by an increase in the contractile parameters. At the skinned fiber level of this transgenic mouse model, 95% replacement of the mouse VLC-1 by the mouse ALC-1 was accompanied by 1.78-fold increase in maximal shortening velocity (V_{max}) compared to the control group (Fewell et al. 1998). On the other hand, it was previously observed that around 20% replacement of the human VLC-1 by the human ALC-1 increased V_{max} of skinned fibres 1.88-fold (Morano et al. 1996).

This functional discrepancy between the human and mouse ALC-1 was supported by a considerable amino acid sequence variation of the atrial essential myosin light chains in both species (Fig. 21). Interestingly, the human-mouse amino acid differences are mostly located at the N-termini of both sequences, with a close similarity between the mouse and rat ALC-1. It has been demonstrated that the amino-terminal domain of the MLC-1 isoforms interacts with the carboxyl-terminal domain of actin (Stepkowski 1995; Sutoh 1982; Timson et al. 1998). This interaction could be of functional importance since inhibition of this interaction using synthetic peptides increased the force production and the shortening velocity of human heart fibers (Morano et al. 1995), which may explain the functional variation in both the human and mouse ALC-1.

Besides the main interest in the molecular therapy of human heart disease, the considerable difference between the human and mouse ALC-1 sequences and function, provided the initiative to undertake this study aiming to characterize, for the first time the effect of human ALC-1 at the intact whole heart contraction level. To achieve this aim, transgenesis was used to direct an essential light chain isoform switch in the rat heart.

Analyzing the morphological data of the transgenic model, no significant difference in the heart weight/bodyweight relationship between the TGR/hALC-1 and control animals was observed, which suggests the absence of hypertrophic response in the hearts of the rat models. Moreover, to confirm the absence of hypertrophy, the expression of alpha-myosin heavy chains, which is essentially down-regulated during hypertrophy (Swynghedauw 1986) was studied by using quantitative Western blot analysis. No change in the expression levels of alpha-MHC in TGR/hALC-1 compared to WKY could be detected.

Human	MAPKKPEPKKEAAKPAPAPAPAPAPAPAPEAPKEPAFDPKSVKIDFTA	50
Mouse	.P.....T....A.P...ASA..E.L***KDS.....S.	46
Rat	.P.....T....V.A...PAP..E.L***RDS.....S.	46
Human	DQIEEFKEAFSLFDRTPTGEMKITYGQCGDVLRALGQNPTNAEVLRLVGK	100
Mouse	96
Rat	96
Human	PKPEEMNVKMLDFETFLPILQHISRNKEQGTYEDFVEGLRVFDKESNGTV	150
MouseSS.T....M.....	146
RatSS.T....M.....	146
Human	MGAELRHVLATLGEKMTAEAEVEQLLAGQEDANGCINYEAFVKHIMSG	197
MouseS.....S.....I...	193
RatS.....T.....V...	193

Figure 21. Amino acid sequence comparison of the human, mouse and rat atrial essential myosin light chains (ALC-1):

Note the significant variability between the human and mouse sequences at the amino termini, which may explain the attenuated ALC-1 function in the mouse compared to the hALC-1. Also a close similarity of the mouse and rat sequences was observed.

A previously published study showed that transgenic overexpression of MLC at high-level results in severe cardiac pathology (James et al. 1999). These findings are in agreement with mine due to the moderate expression levels that were obtained in my TGR/hALC-1 model. However these results stand in opposition to the same author's previous findings, which confirmed the absence of any hypertrophy in the transgenic mice with 95% replacement of the endogenous light chains by the transgene (Fewell et al. 1998).

I observed a significant improvement in the contractile parameters of the 12-24-week old TGR/hALC-1 compared with age-matched WKY animals. Interestingly, aged TGR/hALC-1, especially 36-week old animals, revealed no significant differences in their contractile parameters when compared to age-matched WKY. This normalization of heart function with age could be explained, firstly by the age-dependent attenuation of transgene expression discussed below, and secondly by the age-dependent increase in contractility in the WKY rats, which is in accordance with the findings of previous studies (Nair et al. 2001; Qi et al. 1997).

The 12 weeks old TGR/hALC-1 expressed a reasonable amount of hALC-1 in their ventricles, but a decline in the transgene expression upon aging was observed, that was closely associated with a decline in the improved contractility seen in young TGR/hALC-1. This confirms that the improved contractile functions were associated with the hALC-1 expression. The phenomenon of age-dependent transgene down-regulation was also observed in a previous study using the same α -MHC promoter (Hoffmann et al. 2001). This observation could be due to the attenuation of alpha-MHC expression in WKY rats with age (Morano et al. 1988). I suggest that the improved contractile functions observed in the transgenic rat model were due to the hALC-1 expression rather than to abnormal gene modification(s) caused by random transgene integration. Except for the transgene, there were no obvious changes in the expression levels of the proteins in TGR/hALC-1 compared to the WKY rats as revealed by 2D-proteome analyses. The hALC-1 transgenic protein was localized by immunofluorescence analysis, which showed that hALC-1 was correctly incorporated in-between the Z lines of the sarcomere of the ventricular contractile apparatus.

Furthermore, to confirm the incorporation of the transgenic protein into the ventricular myosin, myosin was purified from the ventricles of transgenic and control rats. An immunoblot for these pure myosin preparations was performed using specific anti-hALC-1 antibodies. The antibodies recognized the transgenic hALC-1 proteins within the purified myosin of the transgenic rat. The persistent existence of the transgenic hALC-1 proteins within the myosin preparation after high ionic strength purification and subsequent ammonium sulfate precipitation suggests that hALC-1 remained incorporated within the myosin. This confirms the correct association of hALC-1 and binding to the ventricular myosin heavy chains.

In a different set of analytical studies using immunofluorescence microscopy, a mosaic pattern of expression for hALC-1 was observed in the cardiomyocytes. These variegated expression patterns have been commonly observed in various transgenic studies in mammals (Dobie et al. 1996; Opsahl et al. 2002).

The MLC-1/ MLC-2 ratio was similar in WKY and TGR/hALC-1 ventricular purified myosin preparations, thus the ectopically expressed hALC-1 replaces the endogenously expressed rat VLC-1 with no net increase in the whole MLC-1 content. These data are compatible with previous results in which different myosin light chains were expressed in human ventricles (Morano et al. 1996) and transgenic mice (Gulick et al. 1997). In 12 weeks-old TGR/hALC-1, I observed around 20% replacement of the rat left ventricular VLC-1 by hALC-1 in purified myosin preparations. Meanwhile, hALC-1 represented about 37% of rat left ventricular whole MLC-1 in whole SDS-soluble transgenic ventricular tissue extracts. Therefore, I suggest that a fraction of the expressed transgene (about 1/3) seems to exist in a free non-bound state in cardiomyocytes.

The moderate replacement of rat VLC-1 by hALC-1 in the 12 weeks-old rat model was accompanied by marked alterations in whole heart mechanics, represented by significant increase in the pressure development, contraction rate, and relaxation rate. These data are consistent with the previous idea that partial replacement of endogenous MLC-1 by hALC-1 is sufficient to improve the contractile functions of the heart (Morano et al. 1996). Furthermore, it is demonstrated that the hALC-1 in rat is more functionally efficient than the corresponding mouse essential myosin light chain isoform in mouse: maximal contraction and relaxation rates were increased by around

100% upon only 20% replacement of endogenous MLC-1 with hALC-1. In contrast, the same functional parameters were only increased by 40-50% upon 95% replacement of mouse VLC-1 by mouse ALC-1. Hence, a moderate expression of hALC-1 could generate a much stronger increase of contractility of perfused intact hearts than an excessive expression of the corresponding mouse ALC-1.

Summary

Most patients with hypertrophic cardiomyopathy and congenital heart diseases express the atrial essential myosin light chains (ALC-1) in their ventricles, partially replacing the ventricular essential light chains (VLC-1). This VLC-1/ALC-1 isoform shift is correlated with an increase in cross-bridge cycling kinetics as measured using chemically skinned fibers from the hypertrophied ventricles of human hearts. To study the functional importance of hALC-1 in the whole intact perfused-heart, a transgenic rat model overexpressing hALC-1 (TGR/hALC-1) in the heart was generated. WKY rats were used as the respective genetically correct control strain.

Using hALC-1_{HIST} protein as a standard, the amount of transgenic protein expression was quantified by Immunoblot analysis of the left ventricular tissue extracts of the transgenic rats. Twelve-week-old TGR/hALC-1 expressed around 17 μ g hALC-1 per mg of whole SDS-soluble protein.

The transgene was localized in-between the Z-lines of the sarcomere by immunofluorescence microscopy. Furthermore, the proper integration of the transgene into the rat ventricular myosin was confirmed by purifying myosin from rat ventricular tissues.

Whole ventricular proteome analysis by 2D-PAGE, resolved approximately 3000 proteins spots in each TGR/hALC-1 and WKY animal. The whole protein expression patterns in both animal groups showed no differences with the exception of the transgenic hALC-1 protein spot.

The perfused heart contractility parameters were evaluated using the Langendorff preparation. Expression of hALC-1 was accompanied by statistically significant improvements ($p < 0.001$) in all measured contractile parameters of the hearts of the TGR/hALC-1 compared to the age matched control (WKY) animals, represented by increases in the developed left ventricular pressure, maximal rate of pressure increase and the relaxation rate. Age dependent decrease in the transgene expression caused a decline of the improved contractility parameters to normal values.

These results demonstrate that the expression of the hALC-1 in the heart not only improved the function of in-vitro preparations, but also of the whole intact organ.

Zusammenfassung

Die meisten Patienten mit hypertropher Kardiomyopathie und kongenitalen Herzerkrankungen exprimieren die atriale essentielle leichte Myosinkette (ALC-1) im Ventrikel, wo sie teilweise die ventrikuläre essentielle leichte Myosinkette (VLC-1) ersetzt. Diese VLC-1/ALC-1 Isoformveränderung korrelierte mit einem Anstieg der Zykluskinetik der Myosin-Querbrücken in chemisch gehäuteten Herzfasern aus hypertrophierten Humanventrikeln. Um die funktionelle Bedeutung der ALC-1 im gesamten intakten Herzen zu untersuchen, habe ich in der vorliegenden Arbeit ein transgenes Rattenmodell charakterisiert, das die humane ALC-1 (hALC-1) im Herzen exprimiert (TGR/hALC-1). WKY-Ratten dienten als genetisch korrekter Kontrollstamm.

Mittels rekombinanter hALC-1 als Standard wurde die exprimierte hALC-1-Menge in SDS-Extrakten linker Ventrikel der TGR/hALC-1 im Western-Blot untersucht. 12 Wochen alte TGR/hALC-1 exprimierten etwa 17 µg hALC-1/mg SDS-Extrakt. Das exprimierte Transgen konnte in der Immunfluoreszenz zwischen den Z-Linien der Sarkomere lokalisiert werden. Die gerichtete Integrations des Transgens in das kardiale Myosinmolekül wurde zusätzlich noch in hochgereinigten Myosinpräparationen nachgewiesen.

Analyse des linksventrikulären Proteoms durch 2D-PAGE, das zur Identifikation von etwa 3000 Proteinen führte, zeigte vergleichbare Proteinmuster in WKY und TGR/hALC-1.

Die Untersuchungen der Kontraktilität des intakten isoliert perfundierten Herzen wurden mit Langendorff-Präparationen durchgeführt. Die Expression des hALC-1-Transgen führte zu statistisch signifikanten ($p < 0.001$) Steigerungen aller gemessenen Kontraktilitätsparameter (linksventrikuläre Druckentwicklung, maximale Geschwindigkeit der Kraftentwicklung, maximale Erschlaffungsgeschwindigkeit). Die altersbedingte Abnahme der Transgenexpression führte zu einer Abnahme der verbesserten Kontraktilitätsparameter auf das Kontrollniveau der WKY-Tiere.

Diese Ergebnisse belegen, dass die Expression der hALC-1 im Herzen nicht nur die Funktion von in vitro-Präparaten, sondern auch die des gesamten intakten Organs zu steigern vermag.

References

- Alyonycheva, T. et al. (1997). Skeletal muscle-specific myosin binding protein-H is expressed in Purkinje fibers of the cardiac conduction system. *Circ Res.* 80: 665-672.
- Arndt, H. et al. (1989). Calcium sensitivity and unloaded shortening velocity of hypertrophied and non-hypertrophied skinned human atrial fibres. *Pflugers Arch.* 415: 209-213.
- Auckland, L. M. et al. (1986). Cardiac myosin light and heavy chain isotypes in tetralogy of Fallot. *Cardiovasc Res.* 20: 828-836.
- Barton, P. J. et al. (1985). The myosin alkali light chain proteins and their genes. *Biochem J.* 231: 249-261.
- Bers, D. M. (2002). Cardiac excitation-contraction coupling. *Nature.* 415: 198-205.
- Bouvagnet, P. et al. (1984). Fiber types and myosin types in human atrial and ventricular myocardium. An anatomical description. *Circ Res.* 55: 794-804.
- Brenner, B. (1988). Effect of Ca²⁺ on cross-bridge turnover kinetics in skinned single rabbit psoas fibers: implications for regulation of muscle contraction. *Proc Natl Acad Sci U S A.* 85: 3265-3269.
- Brodie, B. R. et al. (1977). Effects of sodium nitroprusside on left ventricular diastolic pressure-volume relations. *J Clin Invest.* 59: 59-68.
- Catala, F. et al. (1995). A skeletal muscle-specific enhancer regulated by factors binding to E and CArG boxes is present in the promoter of the mouse myosin light-chain 1A gene. *Mol Cell Biol.* 15: 4585-4596.
- Cohen, C. (1975). The protein switch of muscle contraction. *Sci Am.* 233: 36-45.

Cserjesi, P. et al. (1995). Expression of the novel basic helix-loop-helix gene eHAND in neural crest derivatives and extraembryonic membranes during mouse development. *Dev Biol.* 170: 664-678.

Dantzig, J. A. et al. (1992). Reversal of the cross-bridge force-generating transition by photogeneration of phosphate in rabbit psoas muscle fibres. *J Physiol.* 451: 247-278.

Dobie, K. W. et al. (1996). Variegated transgene expression in mouse mammary gland is determined by the transgene integration locus. *Proc Natl Acad Sci U S A.* 93: 6659-6664.

Eisenberg, E. et al. (1985). Muscle contraction and free energy transduction in biological systems. *Science.* 227: 999-1006.

Fallot, A. (1963). [Contribution to the Pathological Anatomy of Blue Disease (Cardiac Cyanosis)]. *Mars Med.* 100: 779-797.

Fewell, J. G. et al. (1998). Functional significance of cardiac myosin essential light chain isoform switching in transgenic mice. *J Clin Invest.* 101: 2630-2639.

Fodor, W. L. et al. (1989). Human ventricular/slow twitch myosin alkali light chain gene characterization, sequence, and chromosomal location. *J Biol Chem.* 264: 2143-2149.

Geeves, M. A. et al. (1999). Structural mechanism of muscle contraction. *Annu Rev Biochem.* 68: 687-728.

Gordon, A. M. et al. (2000). Regulation of contraction in striated muscle. *Physiol Rev.* 80: 853-924.

Gordon, A. M. et al. (2001). Skeletal and cardiac muscle contractile activation: tropomyosin "rocks and rolls". *News Physiol Sci.* 16: 49-55.

Gorza, L. et al. (1984). Myosin types in the human heart. An immunofluorescence study of normal and hypertrophied atrial and ventricular myocardium. *Circ Res.* 54: 694-702.

Gregorio, C. C. et al. (2000). To the heart of myofibril assembly. *Trends Cell Biol.* 10: 355-362.

Grossman, W. et al. (1972). Alterations in preload and myocardial mechanics in the dog and in man. *Circ Res.* 31: 83-94.

Gulick, J. et al. (1997). Transgenic remodeling of the regulatory myosin light chains in the mammalian heart. *Circ Res.* 80: 655-664.

Haase, H. et al. (1993). Phosphorylation of the L-type calcium channel beta subunit is involved in beta-adrenergic signal transduction in canine myocardium. *FEBS Lett.* 335: 217-222.

Hailstones, D. et al. (1992). Differential regulation of the atrial isoforms of the myosin light chains during striated muscle development. *J Biol Chem.* 267: 23295-23300.

Hayashibara, T. et al. (1994). Binding of the amino-terminal region of myosin alkali 1 light chain to actin and its effect on actin-myosin interaction. *Biochemistry.* 33: 12821-12827.

Helmes, M. et al. (1996). Titin develops restoring force in rat cardiac myocytes. *Circ Res.* 79: 619-626.

Herzberg, O. et al. (1985). Structure of the calcium regulatory muscle protein troponin-C at 2.8 Å resolution. *Nature.* 313: 653-659.

Hirzel, H. O. et al. (1985). Relationship between myosin isoenzyme composition, hemodynamics, and myocardial structure in various forms of human cardiac hypertrophy. *Circ Res.* 57: 729-740.

Hoffmann, S. et al. (2001). Overexpression of the human angiotensin II type 1 receptor in the rat heart augments load induced cardiac hypertrophy. *J Mol Med.* 79: 601-608.

Holmes, K. C. (1997). The swinging lever-arm hypothesis of muscle contraction. *Curr Biol.* 7: R112-118.

Holmes, K. C. et al. (1990). Atomic model of the actin filament. *Nature*. 347: 44-49.

Hopkins, S. C. et al. (1998). Fluorescence polarization transients from rhodamine isomers on the myosin regulatory light chain in skeletal muscle fibers. *Biophys J*. 74: 3093-3110.

Howard, J. et al. (1996). Is the lever arm of myosin a molecular elastic element? *Proc Natl Acad Sci U S A*. 93: 4462-4464.

Huxley, A. F. et al. (1971). Proposed mechanism of force generation in striated muscle. *Nature*. 233: 533-538.

Irving, M. et al. (1995). Tilting of the light-chain region of myosin during step length changes and active force generation in skeletal muscle. *Nature*. 375: 688-691.

Jaenicke, T. et al. (1990). The complete sequence of the human beta-myosin heavy chain gene and a comparative analysis of its product. *Genomics*. 8: 194-206.

James, J. et al. (1999). Transgenic over-expression of a motor protein at high levels results in severe cardiac pathology. *Transgenic Res*. 8: 9-22.

Kabsch, W. et al. (1990). Atomic structure of the actin:DNase I complex. *Nature*. 347: 37-44.

Katz, A. M. (2001). *Physiology of the heart*. Philadelphia, Lippincott Williams & Wilkins xvi, 718.

Klose, J. (1999). Large-gel 2-D electrophoresis. *Methods Mol Biol*. 112: 147-172.

Klose, J. et al. (1995). Two-dimensional electrophoresis of proteins: an updated protocol and implications for a functional analysis of the genome. *Electrophoresis*. 16: 1034-1059.

Kretsinger, R. H. (1980). Structure and evolution of calcium-modulated proteins. *CRC Crit Rev Biochem*. 8: 119-174.

Laemmli, U. K. (1970). Cleavage of structural proteins during the assembly of the head of bacteriophage T4. *Nature*. 227: 680-685.

Langendorff, O. (1895). Untersuchungen am überlebenden Säugethierherzen. *Arch Gesante Physiol*. 61: 291-332.

Linke, W. A. et al. (1997). Actin-titin interaction in cardiac myofibrils: probing a physiological role. *Biophys J*. 73: 905-919.

Lombardi, V. et al. (1995). Elastic distortion of myosin heads and repriming of the working stroke in muscle. *Nature*. 374: 553-555.

Lopez-Lopez, J. R. et al. (1994). Local, stochastic release of Ca²⁺ in voltage-clamped rat heart cells: visualization with confocal microscopy. *J Physiol*. 480 (Pt 1): 21-29.

Lopez-Lopez, J. R. et al. (1995). Local calcium transients triggered by single L-type calcium channel currents in cardiac cells. *Science*. 268: 1042-1045.

Lowey, S. et al. (1971). Light chains from fast and slow muscle myosins. *Nature*. 234: 81-85.

Macera, M. J. et al. (1992). Localization of the gene coding for ventricular myosin regulatory light chain (MYL2) to human chromosome 12q23-q24.3. *Genomics*. 13: 829-831.

Matsuoka, R. et al. (1991). Complete sequence of human cardiac alpha-myosin heavy chain gene and amino acid comparison to other myosins based on structural and functional differences. *Am J Med Genet*. 41: 537-547.

Mercadier, J. J. et al. (1983). Myosin isoenzymes in normal and hypertrophied human ventricular myocardium. *Circ Res*. 53: 52-62.

Milligan, R. A. et al. (1990). Molecular structure of F-actin and location of surface binding sites. *Nature*. 348: 217-221.

Moncman, C. L. et al. (1995). Nebulette: a 107 kD nebulin-like protein in cardiac muscle. *Cell Motil Cytoskeleton*. 32: 205-225.

Moncrief, N. D. et al. (1990). Evolution of EF-hand calcium-modulated proteins. I. Relationships based on amino acid sequences. *J Mol Evol*. 30: 522-562.

Morano, I. (1999). Tuning the human heart molecular motors by myosin light chains. *J Mol Med*. 77: 544-555.

Morano, I. et al. (1997). Changes in essential myosin light chain isoform expression provide a molecular basis for isometric force regulation in the failing human heart. *J Mol Cell Cardiol*. 29: 1177-1187.

Morano, I. et al. (1988). Chronic hypertension changes myosin isoenzyme pattern and decreases myosin phosphorylation in the rat heart. *J Mol Cell Cardiol*. 20: 875-886.

Morano, I. et al. (1995). Myosin light chain-actin interaction regulates cardiac contractility. *Circ Res*. 76: 720-725.

Morano, M. et al. (1996). Regulation of human heart contractility by essential myosin light chain isoforms. *J Clin Invest*. 98: 467-473.

Mornet, D. et al. (1979). The limited tryptic cleavage of chymotryptic S-1: an approach to the characterization of the actin site in myosin heads. *Biochem Biophys Res Commun*. 89: 925-932.

Nair, R. R. et al. (2001). Age-dependent variation in contractility of adult cardiac myocytes. *Int J Biochem Cell Biol*. 33: 119-125.

Offer, G. et al. (1973). A new protein of the thick filaments of vertebrate skeletal myofibrils. Extractions, purification and characterization. *J Mol Biol*. 74: 653-676.

Olson, E. N. (1992). Interplay between proliferation and differentiation within the myogenic lineage. *Dev Biol*. 154: 261-272.

Opsahl, M. L. et al. (2002). Multiple effects of genetic background on variegated transgene expression in mice. *Genetics*. 160: 1107-1112.

Popova, E. et al. (2002). Comparison between PMSG- and FSH-induced superovulation for the generation of transgenic rats. *Mol Reprod Dev*. 63: 177-182.

Popp, D. et al. (1987). Methods of preparing well-orientated sols of f-actin containing filaments suitable for X-ray diffraction. *J Mol Biol*. 197: 679-684.

Popp, D. et al. (1991). X-ray diffraction studies on muscle regulation. *Adv Biophys*. 27: 89-103.

Price, K. M. et al. (1980). Human atrial and ventricular myosin light-chains subunits in the adult and during development. *Biochem J*. 191: 571-580.

Qi, X. L. et al. (1997). Age-dependent changes in the effects of endocardial endothelium on the contractile characteristics of its adjacent myocardium in rats. *J Mol Cell Cardiol*. 29: 823-829.

Rarick, H. M. et al. (1996). An essential myosin light chain peptide induces supramaximal stimulation of cardiac myofibrillar ATPase activity. *J Biol Chem*. 271: 27039-27043.

Rayment, I. et al. (1993). Three-dimensional structure of myosin subfragment-1: a molecular motor. *Science*. 261: 50-58.

Ritter, O. et al. (1999). Expression of atrial myosin light chains but not alpha-myosin heavy chains is correlated in vivo with increased ventricular function in patients with hypertrophic obstructive cardiomyopathy. *J Mol Med*. 77: 677-685.

Saez, L. J. et al. (1987). Human cardiac myosin heavy chain genes and their linkage in the genome. *Nucleic Acids Res*. 15: 5443-5459.

Schaub, M. C. et al. (1998). Modulation of contractility in human cardiac hypertrophy by myosin essential light chain isoforms. *Cardiovasc Res*. 37: 381-404.

Schiaffino, S. et al. (1996). Molecular diversity of myofibrillar proteins: gene regulation and functional significance. *Physiol Rev.* 76: 371-423.

Seharaseyon, J. et al. (1990). Human embryonic/atrial myosin alkali light chain gene: characterization, sequence, and chromosomal location. *Genomics.* 7: 289-293.

Sellers, J. R. et al. (1995). Motor proteins 2: myosin. *Protein Profile.* 2: 1323-1423.

Shevchenko, A. et al. (1996). Mass spectrometric sequencing of proteins silver-stained polyacrylamide gels. *Anal Chem.* 68: 850-858.

Shi, Q. W. et al. (1991). Expression of ventricular myosin subunits in the atria of children with congenital heart malformations. *Circ Res.* 69: 1601-1607.

Small, J. V. et al. (1992). The cytoskeletal lattice of muscle cells. *Eur J Biochem.* 208: 559-572.

Squire, J. M. et al. (1998). A new look at thin filament regulation in vertebrate skeletal muscle. *Faseb J.* 12: 761-771.

Srivastava, D. et al. (1995). A subclass of bHLH proteins required for cardiac morphogenesis. *Science.* 270: 1995-1999.

Srivastava, D. et al. (1997). Regulation of cardiac mesodermal and neural crest development by the bHLH transcription factor, dHAND. *Nat Genet.* 16: 154-160.

Stepkowski, D. (1995). The role of the skeletal muscle myosin light chains N-terminal fragments. *FEBS Lett.* 374: 6-11.

Sussman, M. A. et al. (1994). Tropomodulin in rat cardiac muscle. Localization of protein is independent of messenger RNA distribution during myofibrillar development. *Circ Res.* 75: 221-232.

Sutoh, K. (1982). Identification of myosin-binding sites on the actin sequence. *Biochemistry.* 21: 3654-3661.

Sutsch, G. et al. (1992). Hemodynamic performance and myosin light chain-1 expression of the hypertrophied left ventricle in aortic valve disease before and after valve replacement. *Circ Res.* 70: 1035-1043.

Swynghedauw, B. (1986). Developmental and functional adaptation of contractile proteins in cardiac and skeletal muscles. *Physiol Rev.* 66: 710-771.

Timson, D. J. et al. (1998). The N-terminus of A1-type myosin essential light chains binds actin and modulates myosin motor function. *Eur J Biochem.* 255: 654-662.

Trayer, I. P. et al. (1987). Evidence that the N-terminal region of A1-light chain of myosin interacts directly with the C-terminal region of actin. A proton magnetic resonance study. *Eur J Biochem.* 164: 259-266.

Uyeda, T. Q. et al. (1996). The neck region of the myosin motor domain acts as a lever arm to generate movement. *Proc Natl Acad Sci U S A.* 93: 4459-4464.

Vibert, P. et al. (1997). Steric-model for activation of muscle thin filaments. *J Mol Biol.* 266: 8-14.

Wang, C. et al. (1975). Lowry determination of protein in the presence of Triton X-100. *Anal Biochem.* 63: 414-417.

Winegrad, S. (1999). Cardiac myosin binding protein C. *Circ Res.* 84: 1117-1126.

Woischwill, C. et al. (2004). Regulation of the human atrial essential myosin light chain 1 promoter by Ca²⁺-calmodulin-dependent signaling pathways. *FASEB journal* (submitted).

Xu, C. et al. (1999). Tropomyosin positions in regulated thin filaments revealed by cryoelectron microscopy. *Biophys J.* 77: 985-992.

Zimmermann, K. et al. (1990). Heterogenic mRNAs with an identical protein-coding region of the human embryonic myosin alkali light chain in skeletal muscle cells. *J Mol Biol.* 211: 505-513.

Appendix

PUBLICATIONS

Articles

Abdelaziz AI, Segaric J, Bartsch H, Petzhold D, Schlegel WP, Kott M, Seefeldt I, Klose J, Bader M, Haase H and Morano I. Functional characterization of the human atrial essential myosin light chain (hALC-1) in a transgenic rat model (2004). J. Mol. Med. (IN press).

Abdelaziz AI, Pagel I, Schlegel WP, Kott M, Monti J, Haase H and Morano I. The human atrial myosin light chain (hALC-1) attenuates heart failure (accepted) (2004) Adv. Epx. Med. Biol. (In press).

Abstracts

Abdelaziz AI, Schlegel WP, Kott M, Bader M, Klamm U, Ganten U, Haase H and Morano I. Improved cardiac function by human atrial essential myosin light chain (hALC-1) in a transgenic rat model. J Muscle research and cell motility 24:342 (2003).

CURRICULUM VITAE

Personal Data:

Name: Ahmed Ihab Abdelaziz
 Date of birth: 12/ 11/1971
 Place of birth: Cairo, Egypt
 Nationality: Egyptian
 Marital status: Married
 Work address: Max Delbrueck Center for Molecular Medicine
 Robert Roessle Str.10, 13125,Berlin/Germany
 Home address: Isar Str. 30, 16321,
 Bernau bei Berlin/Germany

 Tel: Work +49 3094062240
 Mobile: +49 15111602053

 Home +49 3338 706752
 Fax: +49 3094062277
 Email: a.abdelaziz@mdc-berlin.de

Education:

March 1998 Medical Practice Licensure by the Egyptian Ministry of Health.
 December 1997 MD, medical degree (MB.B.Ch) Bachelor of Medicine and General Surgery, Ain Shams University–faculty of medicine/Cairo, Egypt.
 January 1990 General Certificate of Education (GCE), University of London, School Examination Board
 1974 – 1990 British School in Cairo (Victoria college) Primary-preparatory & secondary stages of education.

Professional Experience:

- March 2002-Current Researcher at the Max Delbrueck Center For Molecular Medicine, Molecular Muscle Physiology group, Berlin, Germany.
- 1999-2002 Senior house officer (Basic specialist training in Molecular medicine) at the molecular diagnostic labs of Vacsera (Egyptian Institute for Biological products and vaccines) Cairo, Egypt.
- 2001 Intern at the Molecular diagnostic unit of (Alpha) Clinical Diagnostic Laboratory in Cairo.
- 1997 – 1999 House Officer (Internship Rotation) at Ain Shams University Hospitals, Cairo/ Egypt.
- February 1998 Saint George's Hospital (University of London), clinical elective attachment.
- November 1996 Basel University Hospital (Switzerland) clinical elective attachment.

Honours & Scholarships:

- March 2003 Fellow of the Research Training Group (Graduiertenkolleg 754) DFG) at the -Charite medical University/ Berlin, Germany.
- March 2002 Doctorate degree Scholarship from Vacsera, Cairo, Egypt.

Training courses & Programs:

- March 2002-current **Molecular Medicine training program (Wollenberger)** at the MDC/ Berlin, Germany.
- January 2002 **Management training course:** 7 habits of highly effective people by Stephen Covey.
- May 1-4 – 2001 **Bio-safety in Microbiological and Biomedical laboratories-training course** provided by the CDC-NIH (Centres for disease control and prevention, USA).
- May– June 2000 **Molecular Biology training course** at the specialized genetics center (Genetica), Cairo, Egypt.

Scientific invitations & presentations:

- September 2003 **5th PhD Retreat**-invited presentation in Berlin, Germany
- February 2003 **Wollenberger Seminar**-invited seminar speaker at the at Max Delbrueck Center For Molecular medicine/Berlin, Germany, titled (Function of the human ALC-1 In Transgenic Rats)
- November 2002 **King Faisal Heart &Research Centre**-invited presentation /Riyadh, Saudi Arabia, titled (Modulation of myocardial function by Essential Light Chains).
- September 2002 **4th PhD Retreat**-invited presentation in Berlin, Germany.

Linguistic Skills:

English: Fluent, written & spoken

Arabic: Mother tongue

French: Well

ACKNOWLEDGMENTS

First and foremost I would like to thank Prof. Dr. Ingo Morano, who gave me the opportunity to carry out this project, and always supported and encouraged through the time course of my Ph.D. His enormous knowledge, enthusiasm and good mood were my stimulating initiative.

I would also like to thank Dr. Hannelore Haase, Dr. Peter Karczewski and Dr. Michael Bader for their sincere help, advice and valuable discussions during the course of this work. I would like to express my intense and deep gratitude for Dr. Ursula Ganten for the production of the transgenic rats involved in the project.

Special thanks go to Dr. Monika Kott for the immunofluorescence microscopy, Wolfgang-Peter Schlegel for the Langendorff-perfusion and Steffen Lutter for his helpful technical assistance.

I would like to express my sincere thanks to all my lab-mates who shared my daily life, for their help, support and making me feel at home. Special thanks for Christiane Woischwill, Petra Pierschalek, and Daria Petzhold for being very special friends.

I am thankful for the collaboration with the Institute of Human Genetics at the Charité, and I really appreciate the extensive effort made by Jadranka Segaric in performing the whole proteome analysis by 2DE.

Finally, I am grateful for the GraduirtenKolleg (Research Training Group in: myocardial hypertrophy, gene expression & function) -Charité medical University/ Berlin and VACSERA (The Egyptian Org. for Biological Products and Vaccines) for supporting this project.

Erklärung

Hiermit erkläre ich, dass ich die vorliegende Dissertation selbständig und ohne unzulässige Hilfe Dritter angefertigt habe. Die benutzten Hilfsmittel sowie die Literatur sind vollständig angegeben

Berlin, den

Ahmed Ihab Abdelaziz